

A systems approach for monitoring anesthesia

M. Sathyanarayanan

Master of Science Thesis

A systems approach for monitoring anesthesia

MASTER OF SCIENCE THESIS

For the degree of Master of Science in Systems and Control at Delft
University of Technology

M. Sathyanarayanan

November 16, 2021

Faculty of Mechanical, Maritime and Materials Engineering (3mE) · Delft University of
Technology



Copyright © Delft Center for Systems and Control (DCSC)
All rights reserved.



DELFT UNIVERSITY OF TECHNOLOGY
DEPARTMENT OF
DELFT CENTER FOR SYSTEMS AND CONTROL (DCSC)

The undersigned hereby certify that they have read and recommend to the Faculty of
Mechanical, Maritime and Materials Engineering (3mE) for acceptance a thesis
entitled

A SYSTEMS APPROACH FOR
MONITORING ANESTHESIA

by

M. SATHYANARAYANAN

in partial fulfillment of the requirements for the degree of
MASTER OF SCIENCE SYSTEMS AND CONTROL

Dated: November 16, 2021

Supervisor:

dr. S. Pequito

Thesis Committee:

dr. S. Pequito

dr.ing. R. Van de Plas

Abstract

General anesthesia (GA) is an important medical procedure that induces unconsciousness to patients during surgery. Consciousness is a salient feature of the brain, whose neurophysiological features are difficult to be distinguished from unconsciousness. Though it can be defined as an event arising due to interactions in the nervous system, it entirely is not a reliable mechanism. Thus, tracking changes in the brain waves caused by GA is a challenging problem in neuroscience. The exact mechanism to quantify the state of the brain and to distinguish between conscious and unconscious brain is still difficult. Specific features to characterize the state of the brain from the patterns of the brain signal is challenging. Present-day depth of anesthesia monitors index values does not quantify the state of the brain.

An alternative approach is to use dynamical systems theory to assess the underlying dynamics of the brain with imaging technology (e.g., electroencephalographic and electrocorticographic data). Previous results from the literature suggest that stability can play a role in the characterization of unconsciousness. This thesis proposes a detailed study that focus on dynamical systems properties that go beyond stability. In particular, the proposed methodology aims to assess which regions of the brain intervene in the process of consciousness and unconsciousness, as well as quantify how often they interact with each other. Specifically, the approach seeks to leverage the eigenstructure of the underlying approximation of the neural activity captured from intracranial electrocorticographic data.

Our results show that it is possible to differentiate between anesthetic stages of the brain using eigendecomposition. This was possible through a framework that provides a regularised way to sparsify the state estimates of electrocorticographic (ECoG) signal to get a model for analysis of changes in the brain waves affected by GA. Later to look at the eigenvalues and eigenvectors, which gives the frequency of oscillation and direction between different regions of the brain, respectively. It was also observed that the pattern in the evolution of eigenvalues during different anesthetic stages could be able to interpret if the subject was under anesthesia or not.

Table of Contents

Acknowledgements	xi
1 Introduction	1
1-1 Motivation	1
1-2 Research Questions	2
1-3 Research contributions	3
1-4 Thesis outline	5
2 Background information	7
2-1 Anesthesia and Brain	7
2-2 Depth of Anesthesia (DoA) monitors	9
2-3 Control theoretic and stability approaches in monitoring anesthesia	11
2-4 Limitations and gaps in existing work	13
3 Proposed Methodology	15
3-1 Description of experimental dataset	15
3-2 Proposed LASSO regularisation model	17
3-3 Formulation of LASSO regularisation problem in cvx	18
3-4 Eigendecomposition	21
3-5 Evaluation metrics	23
3-6 Analysis pipeline	24
4 Results and discussion	27
4-1 Estimating state matrix (coupling matrix) from the LASSO model	27
4-2 Choosing the tuning parameter β	28
4-3 Eigendecomposition	30
4-4 Discussion	45

5 Conclusion	47
5-1 Limitations	48
5-2 Future work	48
A Sanity checks	49
A-1 Sanity check with neighbouring windows	49
A-2 Sanity check with same amount of sparsity	51
B Supplementary	53
B-1 Effect of same β values	53
C About <code>cvx</code>	55
D Statistical test	57
D-1 Two-sample Kolmogorov-Smirnov test	57
Bibliography	59
Glossary	65
List of Acronyms	65
List of Symbols	65

List of Figures

1-1	<i>Flow chart of an existing model (red shaded) and proposed model (green shaded).</i>	4
1-2	<i>Thesis outline.</i>	5
1-3	<i>Overview of chapters in thesis report.</i>	5
2-1	<i>Four states of brain with their average frequency in Hertz (Hz). Source: medium.com</i>	8
2-2	<i>MRI showing ECoG electrodes in grid array (red). This configuration allows to capture precise brain activity at appropriate physical locations [1].</i>	8
3-1	<i>Different regions of the monkey brain and its functional mapping [2]</i>	16
3-2	<i>Spatial ECoG electrode placement for four monkeys considered for the analysis. Red markers represent the electrodes [3].</i>	17
3-3	<i>Eigenvalue evolution at various stability regimes. (A) shows the plot of example eigenvalues considered whose corresponding evolution (spatiotemporal pattern of oscillations) for the different frequencies are shown in (B) [4].</i>	23
3-4	<i>Analysis pipeline of the proposed methodology.</i>	25
4-1	<i>One-step ahead error plot for different β values in each window for every anesthetic stage of monkey M2. The green line shows the optimal β value chosen for each of the windows considered. The optimal β corresponding to the green line is mentioned. The red markers show the β value of the computed error.</i>	29
4-2	<i>State matrices for each of the anesthetic stages (anesthesia injected, anesthesia start, anesthesia end, recovery start, recovery end) corresponding to the optimal β value in Table 4-2. The x- and y-axis corresponds to the number of channels (128) implanted in monkey M2.</i>	30
4-3	<i>Eigenvalues for the state matrices for β values in Table 4-1 for each of the anesthetic stage.</i>	31
4-4	<i>K-means clusters of eigenvalues in Figure 4-3 for windows given in Table 4-1 in each of the anesthetic stages. The red clusters correspond to cluster 1 representing fast wave oscillations and the blue clusters correspond to cluster 2 representing slow wave oscillations. The x mark represents the centroids of each of the clusters.</i>	32

- 4-5 *Spectral clustering of the eigenvalues of state matrices resulted from the LASSO model based on the frequency and stability (argument and absolute magnitude respectively) of eigenvalue. The coloured dots represent the distribution of eigenvalues from the K-means clustering of different anesthetic stages for monkey M2 with propofol drug. Error bar gives the mean and standard deviation from frequency and stability of each of the clusters. Distribution of cluster points is shown for (A) anesthesia injection vs. anesthesia start, (B) anesthesia start vs. anesthesia end, (C) anesthesia end vs. recovery start, (D) recovery start vs. recovery end.* 33
- 4-6 *Eigenvector of the centroids from K-means clustering for different stages of anesthesia - Monkey M2 with propofol. (A) shows the eigenvalue distribution with 2 clusters (red - cluster1 and blue - cluster2) from K-means clustering, (B) eigenvector of centroid of cluster 1, (C) eigenvector of centroid of cluster 2, visualised on electrode configuration. The colorbar in (B) and (C) represents the normalised eigenvector values.* 35
- 4-7 *Spectral clustering of the eigenvalues of state matrices resulting from LASSO model based on the frequency and stability (argument and absolute magnitude respectively) of eigenvalue. The coloured dots represent the distribution of eigenvalues from the K-means clustering of different anesthetic stages for monkey M1 with propofol drug. Error bar gives the mean and standard deviation from frequency and stability of each of the clusters. Distribution of cluster points is shown for (A) anesthesia injection vs. anesthesia start, (B) anesthesia start vs. anesthesia end, (C) anesthesia end vs. recovery start, (D) recovery start vs. recovery end.* 36
- 4-8 *Eigenvector of the centroids from K-means clustering for different stages of anesthesia - Monkey M1 with propofol. (A) shows the eigenvalue distribution with 2 clusters (red - cluster1 and blue - cluster2) from K-means clustering, (B) eigenvector of centroid of cluster 1, (C) eigenvector of centroid of cluster 2, visualised on monkey M1 electrode configuration. The colorbar in (B) and (C) represents the normalised eigenvector values.* 37
- 4-9 *Spectral clustering of the eigenvalues of state matrices resulting from LASSO model based on the frequency and stability (argument and absolute magnitude respectively) of eigenvalue. The coloured dots represent the distribution of eigenvalues from the K-means clustering of different anesthetic stages for monkey M3 with ketamine-medetomidine drug. Error bar gives the mean and standard deviation from frequency and stability of each of the clusters. Distribution of cluster points is shown for (A) anesthesia injection vs. anesthesia start, (B) anesthesia start vs. anesthesia end, (C) anesthesia end vs. recovery start, (D) recovery start vs. recovery end.* 39
- 4-10 *Eigenvector of the centroids from K-means clustering for different stages of anesthesia - Monkey M3 with ketamine-medetomidine. (A) shows the eigenvalue distribution with 2 clusters (red - cluster1 and blue - cluster2) from K-means clustering, (B) eigenvector of centroid of cluster 1, (C) eigenvector of centroid of cluster 2, visualised on monkey M3 electrode configuration. The colorbar in (B) and (C) represents the normalised eigenvector values.* 40
- 4-11 *Spectral clustering of the eigenvalues of state matrices resulting from the LASSO model based on the frequency and stability (argument and absolute magnitude respectively) of eigenvalue. The coloured dots represent the distribution of eigenvalues from the K-means clustering of different anesthetic stages for monkey M4 with ketamine-medetomidine drug. Error bar gives the mean and standard deviation from frequency and stability of each of the clusters. Distribution of cluster points is shown for (A) anesthesia injection vs. anesthesia start, (B) anesthesia start vs. anesthesia end, (C) anesthesia end vs. recovery start, (D) recovery start vs. recovery end.* 42

4-12	<i>Eigenvector of the centroids from K-means clustering for different stages of anesthesia - Monkey M4 with ketamine-medetomidine. (A) shows the eigenvalue distribution with 2 clusters (red - cluster1 and blue - cluster2) from K-means clustering, (B) eigenvector of centroid of cluster 1, (C) eigenvector of centroid of cluster 2, visualised on monkey M4 electrode configuration. The colorbar in (B) and (C) represents the normalised eigenvector values.</i>	43
A-1	<i>Result for Monkey M2 induced with propofol in anesthesia start stage (window 1501). (A) shows the one-step ahead error plot for β values, with optimal beta β shown with green vertical line. (B) shows the eigenvalue plot from the state matrix of the chosen β in a complex plane. (C) shows the cluster assignments and centroids from K-means clustering and (D) shows the eigenvector plot of the centroids in (C) on monkey M2 electrode configuration.</i>	50
A-2	<i>Plots showing the results with same amount of sparsity induced in LASSO model in Equation 3-7 and from threshold criteria in [5]. (A) shows the eigenvalue (top) and eigen vector plot (bottom) from LASSO model which is tuned using the β parameter to have same amount of sparsity obtained through threshold criteria shown in (B) (top - eigenvalue plot, bottom - eigenvector plot)</i>	51
B-1	<i>Eigenvector of the centroids from K-means clustering for different stages of anesthesia - Monkey M1 with propofol for $\beta = 1000$. (A) shows the eigenvalue distribution with 2 clusters (red - cluster1 and blue - cluster2) from K-means clustering, (B) eigenvector of centroid of cluster 1, (C) eigenvector of centroid of cluster 2, visualised on electrode configuration. The colorbar in (B) and (C) represents the normalised eigenvector values.</i>	54

List of Tables

2-1	<i>BIS score and its corresponding brain states [6].</i>	10
4-1	<i>Optimal β values obtained for respective temporal windows for different stages of anesthesia.</i>	28
4-2	<i>Error values for $\beta = 0$ (least squares) and optimal β for each stage of anesthesia for monkey M2.</i>	28

Acknowledgements

The completion of this thesis marks the end of an incredible two year journey of Masters Systems and Control course at Delft University of Technology. The journey had its ups and downs, where support from many helped me cross all the challenges and hurdles that came along the way. This wouldn't have been possible without few individuals, whom I would like to thank for supporting me in my good and bad days.

First and foremost, I extend my sincere thanks to my supervisor Dr. Sérgio Pequito, for providing me the opportunity to work under him and guiding me throughout this research work. His immense knowledge and plentiful experience constantly encouraged me to explore more. He has been a constant support during my toughest days and gave the best guidance he can which helped me push forward to get the work done. It wouldn't have been possible to complete the thesis on time without his encouragement. Thank you for all the weekly meetings and umpteen number of feedbacks which has helped me give the best every time. I would like to specially thank dr.ing. R. Van de Plas for accepting my invitation for being a part of the thesis committee and for his time.

I express my deepest gratitude to my family and friends whose support and criticism has always helped me become the better version of me. Appa, thanks for trusting me in this process to travel abroad and fulfill my dream. You have been the greatest inspiration all the time to work hard and overstep the bounds. The support and love from my friends is more worth than expressing on paper. Thank you Anisha – for being there for me during the toughest phases I went through. I wouldn't have managed to get up and travel the bumpy road without your phone calls and encouragement. To Shreya – words can't express how grateful for all the fun and good times we had. You are my instant package of enthusiasm, support, encouragement, advice and annoyance. Kavin – thank you for cheering me up always.

Lastly, a special thanks to Ishita and Tanay for sharing their masters journey with me and help me get through the systems and control course.

Delft, University of Technology
November 16, 2021

M. Sathyanarayanan

“In loving memory of my mother”

Chapter 1

Introduction

General Anesthesia (GA) is the state of drug induced sleep-like coma and the most important procedure in a surgical process which puts the patient into an unconscious state [7]. In order to ensure that adequate GA is induced without any overdose, patients are continuously examined for their physiological parameters, heart and oxygen rates [8]. Potential clinical limitations in conventional methods have led to the need for development and exploration of techniques in monitoring anesthesia.

Unconsciousness is identified generally by response such as movement of eyes or response to any stimulation [9]. It is to be noted that clinical unresponsiveness is different from that of unconsciousness, where the former may be caused due to any medical condition and not necessarily through the induction of anesthesia [10]. When GA is underdosed then there are chances that patient recovers from unconsciousness during the surgical procedure or before he is expected to be conscious. On the other hand, overdosage may cause any complications like seizures or even be fatal [11]. Most of these causes of mortality is due to improper drug administration or heart related events [12]. Therefore, anesthetic drug administration is important to keep the patient or subject under GA to be in same state of condition throughout the surgical procedure to ensure that subject is free from any post operative trauma.

1-1 Motivation

For many decades, anesthesiologists relied on the effects of anesthesia on patients to monitor their state of consciousness [3]. For example, they assess heart rate, blood pressure to administer drug dosage. These effects or responses may be related to anesthetic drug. But there is no direct effect that is reflected on the brain [13]. There needs to be a balance between the level of anesthetic drug induced and the state of consciousness of the patient [14]. The state-of-the-art anesthetic dosage level monitors, known as *depth of anesthesia (DoA)* monitors (see Section 2-2), outputs index values by monitoring the brain waves. These scores can be misleading in many cases and thus a robust technique is required to monitor the changes

in the anesthetic stages of the patient. Therefore, anesthesiologists and neuroscientists moved their focus towards deeper behaviour of the brain signals.

Recent research suggests that it is possible to control the anesthesia delivery by robust techniques of control theory [15]. But before, we require modelling of anesthesia monitoring techniques, analysis of brain signals effected by induction of anesthesia. Considering and analysing numerous factors such as multi-variable characteristics, like variation of anesthetic effect among patients, different anesthetic agents and their effects in brain dynamics has, is a challenging problem.

To understand how the brain works, there exists a spatial and temporal neural activity [16]. Spatial resolution may give the information of when a region of the brain was active and temporal resolution gives the information of when the activation took place. The neural activity is captured by techniques like *electrocorticography (ECoG)* and *electroencephalograph (EEG)* using electrodes that measure the difference in potential between two points. The output signals correspond to different frequencies which correspond to different regions of the brain [17]. The ECoG signal activity can be analyzed from the systems point-of-view, which will reveal the spectral characteristics of the dynamics of the brain. In general, we can say that control theory reveals the changes in the input and output associated with the dynamics of the brain. Thus, analysis through system theoretic approach helps to describe the activity of the brain under anesthetic conditions.

Challenge 1: *To develop a model that gives a trade-off between both spatial and temporal aspects of the brain dynamics.*

This thesis work aims at improving the monitoring of anesthesia through a systems approach by distinguishing different stages of anesthesia from the captured brain waves by ECoG. Specifically, the benefits of doing such improvement is that the patient can be avoided from any inter-operative awareness that can cause serious trauma. This improves the monitoring part of the anesthesiologists during the surgical procedure. Since there is no proper definition as how to distinguish the conscious and unconscious states of the brain, a deeper study on the behaviour of the brain under general anesthesia might help. Thus, this work focuses to develop an approach that gives confidence among the anesthesiologists for reliable clinical usage in the future. Furthermore, this research also aims to pinpoint different regions of the brain (spatiotemporal analysis) which are affected during those states.

Challenge 2: *Distinguish between the different anesthetic stages of the brain at a given time using novel control theoretic approaches.*

1-2 Research Questions

Properties of a biological or a natural system, which has been realised through ECoG signals can be fitted to a stochastic time series model. *Auto regressive (AR)* model is such a technique that has been recently used in fields of science and research. AR models have been effectively used to define the oscillations in the system and also to make predictions in a complex system [18]. In [5], the authors have performed linear stability analysis by independently fitting the

time series of short windows to an AR model. After which the stability criteria was given by the drift of eigenvalues, which are obtained from state matrices that were sparsified using a threshold criteria (see Figure 1-1 red shaded region).

Challenge 3: *To regularise the sparsity in the locally linearized model that captures the dynamics of the brain without overfitting.*

The behavioural signatures from EEG by *P. Purdon, E. Pierce et al.* [19], differentiated the loss of consciousness (LOC) and recovery of consciousness (ROC) by analysing a particular frequency of brain waves.

This thesis work aims to propose a model for capturing the brain dynamics in a way that can give signatures through eigendecomposition of the local linearization of the ECoG data collected from monkeys induced with different anesthetic drugs.

Research question: *To find a method to understand the change between the stages of anesthesia, while informing the spatiotemporal behavior using the eigendecomposition that helps to assess the regions of the brain that intervene in the process of consciousness and unconsciousness.*

The green shaded region in Figure 1-1 gives an objective to the following research tasks (RT):

- RT1** : Can a regularised way to sparsify the state matrices of ECoG signals improve the analysis of changes in the brain waves effected by general anesthesia?
- RT2** : Does the proposed method address the trade-off between the sparsity of matrices that allows obtaining similar sparsities to put forward a model which results in better analysis of what is going on.
- RT3** : While aiming to get the preferred model such that changes between the stages of anesthesia is understood, can the problem of overfitting be avoided?
- RT4** : Does considering the magnitude and angle of eigenvalues along with the eigenvectors, contribute in distinguishing signatures for different stages of anesthesia?
- RT5** : Does the proposed method performs well in its objective to capture the dynamics of the brain than the existing method in literature?

1-3 Research contributions

The method of estimating the state matrix by local approximation of linear dynamics of the data and tuning the level of sparsity by using *least absolute shrinkage and selection operator (LASSO)*, to the best of the writer's knowledge has not been formulated before in the literature. This work aims to pinpoint the regions of the brain active during the different stages of anesthesia, which will help the anesthesiologists to see if the subject has entered the

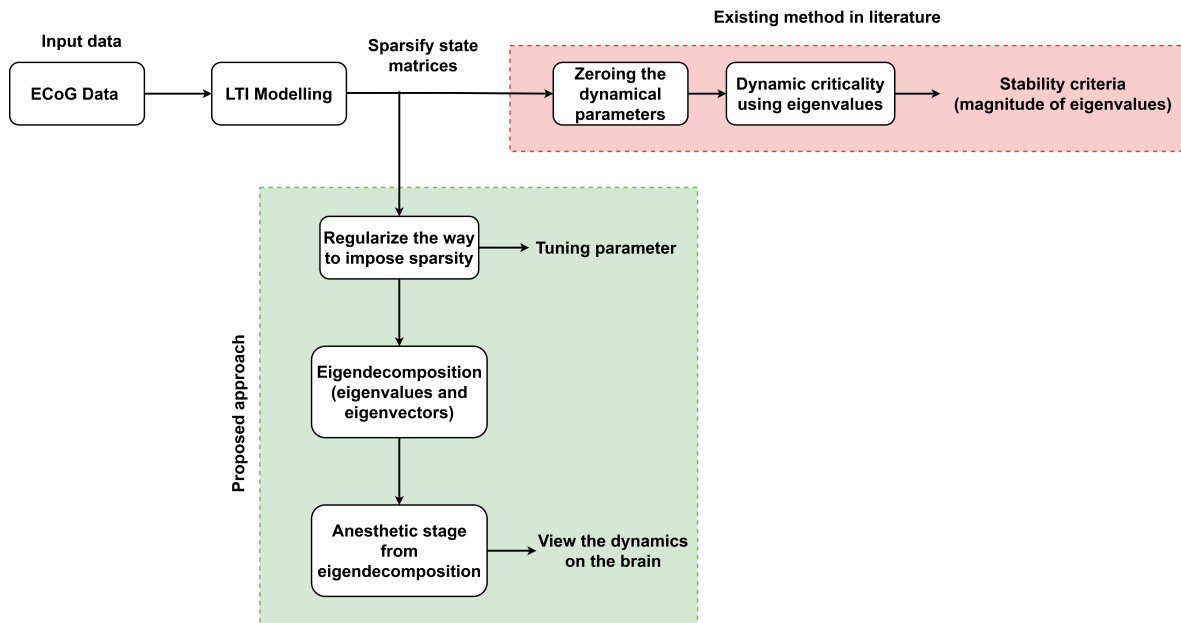


Figure 1-1: Flow chart of an existing model (red shaded) and proposed model (green shaded).

anesthetic stages or not. The result gives the active electrode map on the brain montage, which gives the feel of looking at the brain regions, rather than looking at the raw ECoG signals.

This work contributes in formulating a method that regularises the way in which the state matrix is sparsified without any threshold criteria, rather uses a penalty term, i.e., a tuning parameter, to find the optimized amount of sparsity for capturing the brain dynamics. Also, the analysis is carried out using the eigenvectors as well. These eigenvectors of the corresponding eigenvalues are visualized on the brain image with the location of electrodes. The obtained results are reliable as the estimates of the state matrices are sparsified in a way to filter important information, since the eigenvectors chosen depends on the eigenvalues which are obtained from the state matrix.

The eigenmode decomposition can be effectively used which may help in interpreting how spatiotemporal characteristics evolve over time. The spatial analysis will better help in understanding which regions of the brain is affected or is crucial under anesthesia. Enhancing the time evolution of eigendecomposition is important, as the eigenvalue-eigenvector pairs captures various linearly independent dynamical spatiotemporal process [20].

1-4 Thesis outline

The thesis report structured in the following way.

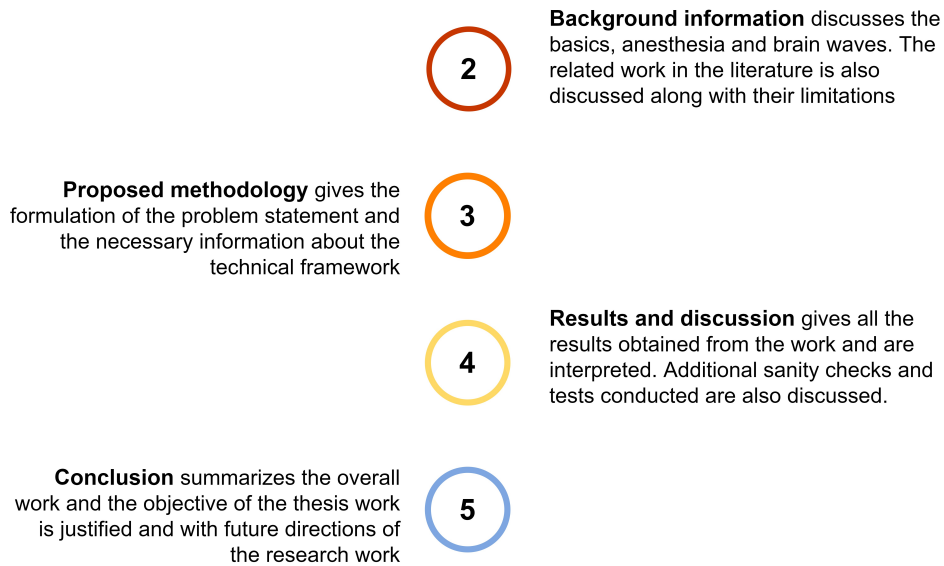


Figure 1-2: Thesis outline.

A more detailed overview of the thesis structure is illustrated in Figure 1-3. The purple boxes represent the chapters whereas the orange boxes represents the research methodologies and their outcomes.

Chapter 1 Introduction	Chapter 2 Background information	Chapter 3 Proposed Methodology	Chapter 4 Results and Discussion	Chapter 5 Conclusion
Basics on anesthesia, brain and ECoG signals	Least squares and LASSO regularisation	Results from LASSO and comparison with Least squares approach		Limitations
Literature Review	Formulation of LASSO problem in cvx	Eigen decomposition and clustering	Future recommendations	
Limitations and gaps in the existing literature work	Eigendecomposition	Validation tests	Personal implications	

Figure 1-3: Overview of chapters in thesis report.

Background information

This chapter briefly introduces the basics of anesthesia and brain waves to help the reader have the knowledge on some related terms used later in this report. Further this chapter discusses about the related work in the literature for modelling of brain ECoG signals. Also, the previous work on stability analysis relating to monitoring of anesthesia is discussed. Each of the literature work discussed is accompanied by its limitations that lead to the foundation of the proposed methodology.

2-1 Anesthesia and Brain

A basic understanding of how a brain works and is effected by induction of anesthesia is necessary in order for any investigation or analysis of related data and behaviour. The brain is a part of the *central nervous system (CNS)*, which has three main parts namely: the cerebrum, cerebellum and brain stem. The largest part of the brain is cerebrum and has two halves: the right and left hemispheres [21]. These cerebral hemispheres are divided into four main lobes: frontal, parietal, occipital and temporal.

Our focus in this thesis work will be entirely towards general anesthesia, which can be induced intravenously or intramuscularly [22]. Upon induction of anesthesia, it affects electrical activity of the brain, displayed by brain states or brainwaves. The brainwaves are electrical impulses that can be measured using EEG or ECoG. These electrical impulses occur at various frequencies which can be classified as four bands as shown in Figure 2-1: beta (12-27 Hz), alpha (8-12 Hz), theta (3-8 Hz) and delta (0.2-3 Hz) (in the order of low amplitude to high amplitude respectively) [23]. However, these conventional alpha, beta, theta and delta bands are not associated with smaller regions of the cortical area, which are found to exhibit additional intrinsic frequency oscillations [24].

The ECoG recordings show additional frequencies while the patient is at rest and awake. Seven types of oscillations are predominant with peaks at 3-5 Hz, 7 Hz (narrow band), 7 Hz (broad band), 10 and 17 Hz [24]. These frequencies largely correlate with the conventional

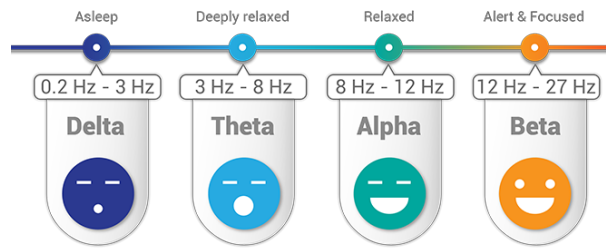


Figure 2-1: Four states of brain with their average frequency in Hertz (Hz). Source: medium.com

bands and found to be distributed throughout different brain regions, with 7 Hz being a predominant frequency [24].

As mentioned earlier, general anesthesia affects some key regions of CNS, which means that it can manipulate its functioning or behaviour. It is important to be noted that most transitions were noted near the cortex surface and in thalamus nuclei [9]. In this way of tracking the behaviour of the brain activity in terms of transitions, researchers are finding some alterations in an anesthetized brain. According to Emery Brown, an anesthesiologist and neuroscientist, anesthesia effects the brain circuits from communicating with each other, which results in unconsciousness [7]. Anesthesia alters brain activity by targeting the neuro-receptors, which are responsible for the transfer of information between neurons [8].

Neuroimaging: Electrocorticography (ECoG) vs. Electroencephalography (EEG)

The changes in brain activity can be measured using non-invasive (EEG) or invasive (ECoG) techniques to collect the brain signals and analyse data further [25]. EEG is a commonly used neuro-imaging technique, for example in treatment for epilepsy and to understand epileptic phenomena. EEG has poor spatial, excellent temporal resolution and very low signal to noise ratio with poor sensitivity to higher frequencies [26]. On the other hand, ECoG has high spatial and temporal resolution and less susceptible to artefacts in contrast to EEG [27]. A possible electrode placement and configuration of ECoG is shown in Figure 2-2.

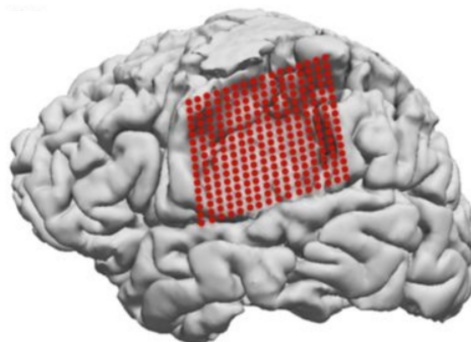


Figure 2-2: MRI showing ECoG electrodes in grid array (red). This configuration allows to capture precise brain activity at appropriate physical locations [1].

ECoG is measured by using electrodes that are subdurally implanted to the brain surface (i.e., the electrodes are placed on the surface of the cortex). Whereas, in EEG the signals

are measured from the surface of the head. The electrodes are non-invasive and can be placed on the scalp using some adhesive. So, EEG does not depend on the region specific signals like implanted ECoG electrodes, rather they capture brain activity changes above the skull [28]. This results in smaller amplitude signals and lesser frequency components in EEG than recorded in ECoG, since the signals get attenuated by tissues and skull [29].

Raw ECoG data is said to contain more information than raw EEG data. When GA is induced, significant changes in the EEG or ECoG signals can be noted. These oscillations may help in differentiating awake and anesthetized states from the recordings.

ECoG recording is carried out by placing an array or patch of electrodes on the surface of the cortex. It is generally a 64 or 128 electrode configuration, that will be implanted on the surface of the cortex (see Figure 2-2). Unlike EEG having a high temporal resolution, ECoG additionally has relatively high spatial resolution [30]. ECoG has significant improvement in the localisation of electrical activity. It also effectively captures higher frequency components of the signal.

In this thesis, the data utilized for analysis is the ECoG data recorded from monkeys (more information about signal recordings in Chapter 3 under methods and materials).

Anesthetic agents

Anesthetic agents are used to induce unconsciousness and are classified into intravenous and inhalational anesthetic agents [31]. Intravenous agents are injected into the patients, as sedatives or narcotics. With these anesthetic agents the loss of consciousness (depth of anesthesia) is achieved immediately. It is to be noted that the effect of anesthetic drugs varies among patients of different age and gender [30].

Propofol is the most commonly used intravenous sedative [32]. Ketamine is also another sedative which is an old anesthetic agent but still in clinical use. Sevoflurane is the commonly used inhalational anesthetic agent for mainly spine surgeries.

2-2 Depth of Anesthesia (DoA) monitors

For many decades, anesthesiologists relied on the effects of anesthesia on patients to monitor their state of consciousness. For example, they assess heart rate, blood pressure to administer drug dosage. These effects or responses may be related to anesthetic drug. But there is no direct effect that is reflected on the brain [13]. There needs to be a balance between the level of anesthetic drug induced and the state of consciousness of the patient [14]. There are many DoA monitors used for clinical purposes but the most used method is the *Bispectral (BIS)* index. This is the first EEG based quantitative monitor clinically used to monitor DoA [33].

Bispectral analysis

The term bispectral denotes phase and power relationship between any two EEG frequencies. These monitors process the EEG data for any spontaneous electrical activity in the brain [13].

BIS is used as a tool to predict the level of hypnosis, derived from EEG data. It was developed for the purpose to reduce any risk of trauma caused due to wakefulness during a surgical procedure under anesthesia. When the patient is awake, the electrical activity captured in EEG is seen as a small amplitude and high frequency. Under various (most) anesthetic dosage, the EEG signals vary as follows. Initially, the EEG signals show an increased amplitude and with increased dosage the frequency is reduced. At deeper levels, the EEG becomes flat with bursts at some periods, which is referred to as isoelectric EEG [6].

The BIS algorithm uses a statistical approach to analyse the measured EEG data and computes a number between 0-100, commonly called as BIS score. These values are not measurements but rather an indication of changes in the state of brain under anesthesia. BIS score of 0 refers to the isoelectric EEG and a score of 40 to 60 refers to surgical anesthesia. Table 2-1 shows the list of BIS scores and their corresponding brain state. The algorithm is not based on any physical equation or laws, but rather considering empirical medical evidence. The algorithm uses frequency versus power spectrum of EEG and the synchronization of the EEG over time, to predict the index value [6].

BIS score	Brain state
100	Awake
80	Light to moderate sedation
40-60	General anesthesia
40	Hypnotic
20	Burst suppression
0	Flat line

Table 2-1: *BIS score and its corresponding brain states [6].*

Synchronization in EEG is the in-phase sine wave component of the signal. Anesthesia effects this by increasing the degree of synchronisation [6]. To measure the degree of synchronization, analysis on phase component is needed in addition to power and frequency.

Limitations of bispectral index algorithm

The response time of EEG is slow from 25 seconds to 4 minutes. As a result, the event of a patient recovering from anesthesia will be known with a considerable delay. The wakefulness of the patient can happen before the monitor indicates the respective BIS score. This can be a serious issue on inter-operative awareness, where the patient recovers from anesthesia during surgery [6].

The anesthetic agents also play a role in its performance. Mostly, it is accurate for both intravenous and inhalational anesthetic drugs. But anesthetic drugs like ketamine gives a different EEG signal, which eventually puts a limitation on BIS score. Every patient shows different EEG responses to different anesthetic doses and BIS algorithm does not give a value of threshold to indicate a patients' loss of consciousness [34]. BIS score can mislead in at least 5 percent of the patients, due to the presence of artefacts captured by the EEG. If the BIS algorithm is designed to be prone to artefacts, consider the type of anesthetic dose given and increase the response time, it may be a reliable tool [6].

2-3 Control theoretic and stability approaches in monitoring anesthesia

Emerging technologies and major researches in control engineering and neuroscience have paved way for more accurate measurement and analysis of the loss of consciousness. The existing monitors have not effectively related to the loss of consciousness and also has its own disadvantages making it less reliable for clinical use. This section discusses the alternative methodologies in literature, to assess the brain state as a dynamical system that needs to be appropriately monitored under such situations. Many theoretical and practical exploration reveal that statistical analysis gives the relationship between conscious and unconscious states [35]. The brain is a complex system, and hence the signals recorded from it through EEG or ECoG is dynamical in nature. Awake versus the anesthetized states are captured by the spectral properties of the dynamical system [36].

Dynamical criticality

Complex systems are found to exhibit stable and unstable dynamic conditions. When systems possess the property to be dynamic between stability and instability, they attain higher levels of computational properties [37]. This is called as criticality hypothesis. Dynamic criticality is also termed as 'the edge of chaos'. At this point, we might recall the definitions of stable and unstable in dynamical systems.

A stable system is one where the oscillations are regular and stationary states remain the same over time. If an asymptotically stable system is subject to little perturbation, its effect on the overall system dies out. By which, stable or ordered systems are robust to perturbations. An unstable system is one where any tiny perturbation will affect the system and the steady states do not have a regular pattern over time [37].

A critical system is said to be a mixture of both stable and unstable systems mentioned above. When the system is subject to perturbations, the effect will remain constant. In neuroscience, dynamical criticality means managing the change in dynamics steadily and quickly when it approaches the critical point [38]. When changes in the neural systems are caused by the input, in our case, anesthesia, will require to balance between the stable and unstable modes quickly in a short span. The neural signals captured by EEG and ECoG provides a way to understand brain activity.

Linear time-invariant (LTI) approach

ECoG and EEG signals are time series data. Properties of a biological or a natural system, which has been realised through these techniques can be fitted to a stochastic time series model. Auto regressive (AR) model is such a technique that has been recently used in fields of science and research. AR models have been effectively used to define the oscillations in the system and also to make predictions in a complex system [18]. Equation 2-1 gives the definition of autoregressive model $y(n) \in \mathbb{R}^m$,

$$y_n = \sum_{i=1}^p \mathbf{A}(t) y_{n-i} + e_n \quad (2-1)$$

where n is the number of steps of discrete time series, p being the order of the model, $\mathbf{A}(t) \in \mathbb{R}^{m \times m}$ is a coefficient parameter of AR matrix (square matrix) and e is the error term (column vector) [18]. State matrix \mathbf{A} gives a relationship between the current state of y_n with all the previous values y_{n-1} [18]. The parameters of the AR model can be fit into an observed time series data. This way the dynamics of that system can be converted as the parameters of the AR model.

Autoregressive model for dynamics of brain

The brain is highly nonlinear and literature contains fitting the AR model to its dynamics. ECoG can be described by a single AR model of any order of choice, for the entire time series [18]. ECoG being multivariate time series, which means that it depends on other values in addition to past values of $y(n)$, to predict the future values of the variable. Linear stability analysis can be carried out by independently fitting the time series of short windows to a AR model [5]. In [5], the authors studied the stability properties during the loss of consciousness with ECoG data from monkeys, have implemented fitting the AR model with short time windows.

Local approximation of dynamics of the system in those short temporal windows $V(n)$, can be done using AR modelling [5], [18]. $V(n)$ is a column vector, of dimension N_e which denotes the number of channels in the ECoG recording and n is the number of steps in time t , given as $n = t \times F_s$, where F_s is the sampling frequency. For each of the windows, the eigenmodes and the absolute value of eigenvalues (stability parameter) of state matrix A gives useful information for further stability analyses. These eigenmodes are estimated from the short windows of size $V(n)$ at time t . This gives the local approximation of the time series window to fit in the AR model given by Equation 2-2 [18],

$$\mathbf{y}_{n+1} = \mathbf{A}(t)\mathbf{y}_n + \mathbf{e}_n \quad (2-2)$$

where \mathbf{y}_n is the time series from n steps, $\mathbf{A}(t)$ is the state matrix containing the coefficients of size $N_e \times N_e$ and e is the noise vector [18]. The estimates of matrix \mathbf{A} at every n time step can be estimated by least squares algorithm, see for instance [39]. The estimation is carried out by representing the first order AR model (i.e., AR(1)), in the form of an ordinary regression model. In [18], it is provided evidence that the extracted eigenmodes capture the critically dynamic system having a Hopf bifurcation.

The autoregressive matrices were simplified and binarized by estimating the mean and standard deviation of the matrix value distribution. The resulting matrix was known as the summary matrix. Another matrix was constructed with this summary matrix, say S_{ij} to capture the diagonal and off-diagonal effects of the autoregressive matrix. The value of the diagonal element was higher when the subject was awakened [5].

Eigenmode decomposition

The temporal dynamics can be inferred from the eigenmodes of \mathbf{A} of the AR(1) model. One of the major advantages of using an AR model fitting is that the stability of the underlying system can be understood from the eigenvalues (λ) of matrix \mathbf{A} or evolution matrix [39]. The mode is said to be asymptotically stable, if $|\lambda| < 1$ and unstable if $|\lambda| > 1$. The former tends to zero by time (damping) while the unstable modes might explode or grow exponentially over time [5]. If the eigenvalues are complex, then they have a frequency of oscillation for the eigenmodes which is given by $f_\lambda = F_s |\arg \lambda| / (2\pi)$, where F_s is the sampling frequency [18].

When $|\lambda| = 1$, then criticality corresponds to the point at the transition between (asymptotically) stable and unstable modes [5]. Thus, stability of the dynamics can be said to be between the exponential growth and decay along the direction of the corresponding eigenvector. So, linear stability analysis could be carried out using the autoregressive model of the ECoG time series data instead of reconstructing the dynamics of the system.

Stability and criticality under the induction of anesthesia

Induction of anesthesia can be related to the changes in dynamics of the brain. It has been noticed that the cortical dynamics stabilize after the induction of anesthesia [5]. In [5], the cortical dynamics stabilization was studied for anesthetic drugs namely, propofol and ketamine-medetomidine dosages, on four different monkeys.

The criticality indices at different stages of anesthesia: before drug administration, during induction and after recovery was studied. The state matrices of the system model was sparsified (zeroing few entries) using a threshold criteria and their corresponding eigenvalues were found. The criticality modes (eigenvalue $\lambda = 1$) were found to be crowded near value 1 of unit circle, during awake and at the time when anesthesia was induced. During the effect of anesthesia, the criticality modes were found to be decreasing. The criticality modes at 1 were no longer dense within 4 minutes of induction. The index value decreased approximately to about 13% from 17%. The decrease is seen below 0.98, and it can be considered as a threshold value arbitrarily. Thus, after the induction of anesthesia the dynamic criticality which is observed during awake is vanished [18], [5].

2-4 Limitations and gaps in existing work

Unconsciousness caused by induction of general anesthesia has no reliable method to be distinguished from awake or conscious state, with respect to brain activity. The distinguishing property between conscious and unconscious states is still unknown and is highly in debate question in the field of neuroscience. Proving that there exists one has been very difficult because there was no significant signatures or feature that reflect consciousness or enough mentioning about in terms of brain activity.

Despite anesthesiologists having experience with awareness and about the amount of anesthetic dosage to be induced, the procedure to find if the patient might recover from unconsciousness still remains imperfect. Definition of consciousness is yet to be quantified by some

theory and the fact that different anesthetic drugs acts differently on individual patients add additional limitations.

Capturing the dynamics of the brain from its spectral characteristics is a conventional method [40]. The use of dynamical stability to distinguish between the conscious states of the brain was more superior to the results obtained from the spectral information of the signal [41]. It is to be noted that the dynamical stability also increased when the temporal window size was increased. Thus, linear stability analysis of ECoG data, not only brings out the individual signal characteristics, but also the behaviour and changes in the interactions of the cortical regions of the brain, that result in the brain signals.

In the context of dynamical stability, the most important factor in systems theory is that the dynamics are strongly influenced by linearity [5]. But when the system is dynamically critical, this is highly non-linear. Within the analyses of [5], where the findings suggest that most of the eigenvalues lie in the critical regime, meaning that the system cannot be predicted in the long run, as the linear approximation changes. The study can only say how the system moves within the stable and dynamically stable regions.

The dynamic nature of the brain is critical in the formulation of control objectives for stability analysis to assess the stable and unstable regimes under the induction of general anesthesia, in different regions of the brain at different times. Development of methods or algorithms for better performance and that deals with constraints need to be studied and analysed.

Enhancing the time evolution of eigendecomposition is important, as the eigenvalue-eigenvector pairs capture various linearly independent dynamical spatio-temporal processes [20]. The following chapter discusses the proposed methodology and how the eigenvalues and eigenvectors can be effectively utilised to capture the dynamics of the brain.

Proposed Methodology

This chapter provides the materials and methods, i.e., the dataset used for analysis and the proposed methodology over the existing work, respectively. The chapter introduces the proposed method to monitor anesthesia using LASSO and effectively utilize the eigendecomposition in capturing the dynamics. Also, the reader is introduced to the required terms or metrics to be known for the later part of the report.

3-1 Description of experimental dataset

This research is mainly focused on the data that is acquired from the ECoG electrodes captured with different types of anesthesia. At the laboratory for Adaptive Intelligence, Brain Science Institute, data was collected from four different monkeys for two different types of anesthesia. These datasets were acquired from the public server Neurotycho <http://www.neurotycho.org/> [42]. These ECoG time series data were recorded during awake, anesthetic and sleeping conditions. The ECoG time series data consists of 128 channels (rows in .mat file) and the data was collected under different anesthetic dosages which are propofol, ketamine and medetomidine. The available data also has the time when the anesthesia was induced, anesthesia start and recovery time, which is helpful to cross verify during the analysis. The data was also used in the research work [5], [43], hence can be considered reliable for this thesis.

The electrodes were placed at a distance of 5mm on the left hemisphere of the brain, covering the major lobes frontal, parietal, temporal and occipital (see Figures 3-1 and 3-2). All the data were filtered using a non-causal notch filter to remove harmonics at 50 Hz and bandpass filtered between 5 and 500 Hz [42]. The available data is found to be filtered when checked with MATLAB using 'idealfilter' function. Thus, the data available was directly used for analysis. The data is provided with the time when the subject was in different stages of anesthesia. Thus, this is useful for segmenting the windows.

Regions of monkey brain and electrode placement

Since the dataset is obtained from the monkeys, knowledge about the region of the monkey brain and the activities associated with it is required. The structure of the monkey brain is slightly different from that of the human brain (discussed in Section 2-1), so the knowledge about activities associated with the regions of the monkey brain will help in analysing the different stages of anesthesia from the results. Figure 3-1 shows the functional regions of the brain of a monkey.

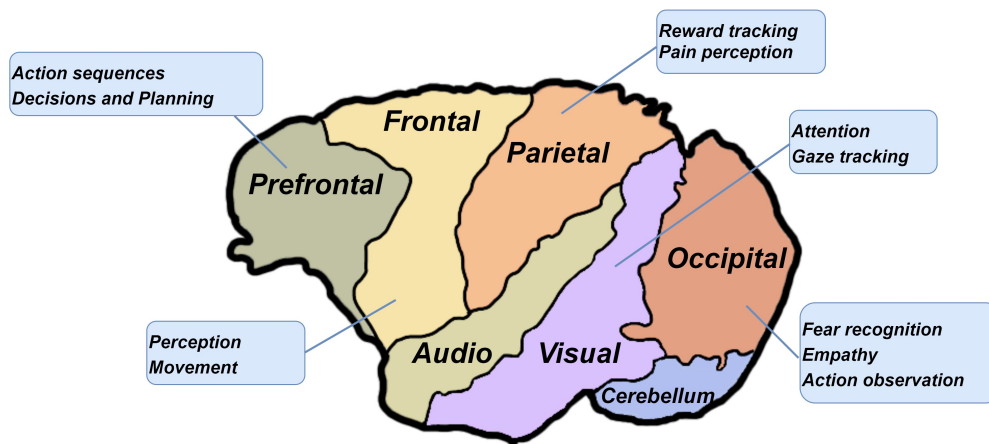


Figure 3-1: Different regions of the monkey brain and its functional mapping [2]

The monkey brain has four cortical regions: frontal cortex, temporal cortex, parietal cortex and motor cortex. The temporal cortex is divided into audio and visual cortex [44]. The functional activities of these cortical regions as follows:

- **Frontal cortex:** Includes any movement in the thighs, legs, toes and foot. This region also includes the movements in the arms and fingers, also the face muscles.
- **Prefrontal cortex:** This region is responsible for the action sequences, action observation, decisions and planning [45].
- **Temporal visual:** Responsible for the learning perception, object recognition and aversion. It is also responsible for gaze tracking and attention.
- **Temporal audio:** To process the sequences of sounds, without which the monkeys find difficulty in recognising different frequencies of sounds to communicate between each other [46].

- **Parietal cortex:** This cortex relates mostly to the senses the monkey can feel such as the touch sensation like temperatures and pain.
- **Occipital:** This region is responsible for action observation and fear recognition.

The placement of the ECoG electrodes on four different monkeys ($M1$, $M2$, $M3$, $M4$) is shown in Figure 3-2 [42]. The data was collected by placing the electrodes in a way that covers all the regions of the monkey brain. This data is thus completely reliable for the analysis as it will give a better interpretation of brain dynamics.

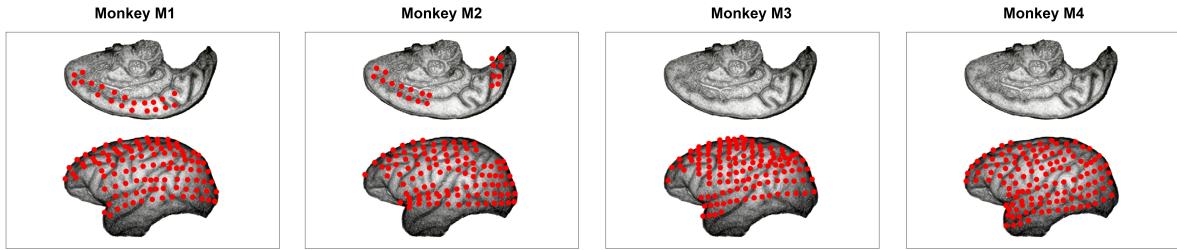


Figure 3-2: Spatial ECoG electrode placement for four monkeys considered for the analysis. Red markers represent the electrodes [3].

3-2 Proposed LASSO regularisation model

LASSO extends as least absolute shrinkage and selection operator. This model introduces a penalty term to the magnitude of the coefficient to be minimised. LASSO is regularisation method that can induce sparsity to the models. The proposed methodology has a regularised way to impose sparsity to the \mathbf{A} matrix instead of using some threshold criteria. Thus, the absolute values of weights will be (in general) reduced, and many will tend to be zeros. The penalty term has a tuning parameter beta (β) that is multiplied to norm-1 of the parameters that we seek to sparsify (L1 regularisation).

This penalty constraint lowers the size of some of the absolute values coefficients and leads to some features having a coefficient of 0, essentially dropping it from the model. This way, it is also a form of filtering the features and results with a model that is simpler and more interpretable.

The LASSO method aims to produce a model that has high accuracy and only uses a subset of the original features by penalizing the coefficients and dropping it off which improves the model.

The following allows to understand the evolution of a least squares problem to a LASSO model. Equation 3-1 gives the least squares model to minimize the state matrix \mathbf{A} (or coupling matrix).

$$\min_{\mathbf{A}} \|X_{k+1} - X_k * \mathbf{A}\|^2 \quad (3-1)$$

where X_k is the ECoG data on the k^{th} step and X_{k+1} is the ECoG data point on the $k + 1^{th}$ step. To induce sparsity to the \mathbf{A} matrix, this model is added with a regularisation term $\beta * \|\mathbf{A}\|_0$, where $\beta \geq 0$ is the tuning parameter that adds the penalty. So the problem now can be read as in Equation 3-2,

$$\min_{\mathbf{A}} \|X_{k+1} - X_k * \mathbf{A}\|^2 + \beta * \|\mathbf{A}\|_0 \quad (3-2)$$

The above problem with the 0-quasi-norm is difficult to solve since the regularisation term is a non-convex optimization problem. Replacing the quasi-norm with norm-1 forms the LASSO problem as given in Equation 3-3,

$$\min_{\mathbf{A}} \underbrace{\|X_{k+1} - X_k * \mathbf{A}\|^2}_{\text{sum of squares}} + \underbrace{\beta * \|\mathbf{A}\|_1}_{\text{LASSO penalty}} \quad (3-3)$$

The norm-1 is a convex problem and the sum of least squares is again convex. And thus the LASSO problem in Equation 3-3 is a convex optimization problem. Therefore, there is a global minimum, but the LASSO problem is not strictly convex [47]. Therefore, the β parameter can have many values that accounts to minimise the objective. In this thesis, LASSO problem is implemented using `cvx` in MATLAB (see Appendix C). The formulation of Equation 3-3 from the LTI model is described in the below section.

3-3 Formulation of LASSO regularisation problem in `cvx`

The data consists of 128 channels, i.e., 128 electrodes and measured time are in milliseconds (ms). Therefore, the rows of the ECoG data matrix (m) = 128. The given data matrix is split into number of windows of size $500 ms$ non - overlapping windows. Each of these temporal windows needs to be fit into the model. The following equations describe the formulation of Equation 3-3 for one of the windows, k .

The dimension of the temporal window of the ECoG data matrix is 128×500 and $(X, b) = (X_k, X_{k+1})$.

$$\left[\begin{array}{c} DATA \\ \end{array} \right]_{128 \times 500}$$

The LTI model to fit the ECoG potentials using least squares for each window is given by,

$$\underbrace{X_{k+1}}_b = \mathbf{A} \underbrace{X_k}_X + \varepsilon_k \quad (3-4)$$

Since the number of channels in the ECoG array is 128 (i.e., 128 rows), the above equation can be written as follows,

$$\begin{aligned}
[X_{k+1}^1] &= \left[\begin{array}{c} a_1 \\ \vdots \\ a_{128} \end{array} \right]_{1 \times 128} \left[\begin{array}{c} X_k \\ \vdots \\ X_k \end{array} \right]_{128 \times 1} \\
[X_{k+1}^2] &= \left[\begin{array}{c} a_2 \\ \vdots \\ a_{128} \end{array} \right]_{1 \times 128} \left[\begin{array}{c} X_k \\ \vdots \\ X_k \end{array} \right]_{128 \times 1} \\
&\vdots \\
[X_{k+1}^{128}] &= \left[\begin{array}{c} a_{128} \\ \vdots \\ a_{128} \end{array} \right]_{1 \times 128} \left[\begin{array}{c} X_k \\ \vdots \\ X_k \end{array} \right]_{128 \times 1}
\end{aligned}$$

for all $k = 0, \dots, 499$, corresponds to the size of the window. Here a_i , where $i = 1 \dots 128$, is the rows of the state matrix corresponding to each of the channels of the ECoG array in monkey. X_{k+1}^i is a scalar (poles of the scalar will be a scalar again). Now taking transpose,

$$\begin{aligned}
[X_{k+1}^1]^\top &= \left[\begin{array}{c} a_1 \\ \vdots \\ a_{128} \end{array} \right]_{1 \times 128} \left[\begin{array}{c} X_k \\ \vdots \\ X_k \end{array} \right]_{128 \times 1} \\
[X_{k+1}^2]^\top &= \left[\begin{array}{c} a_2 \\ \vdots \\ a_{128} \end{array} \right]_{1 \times 128} \left[\begin{array}{c} X_k \\ \vdots \\ X_k \end{array} \right]_{128 \times 1} \\
&\vdots \\
\underbrace{[X_{k+1}^{128}]^\top}_b &= \underbrace{\left[\begin{array}{c} a_{128} \\ \vdots \\ a_{128} \end{array} \right]_{1 \times 128}}_A \underbrace{\left[\begin{array}{c} X_k \\ \vdots \\ X_k \end{array} \right]_{128 \times 1}}_x
\end{aligned}$$

for all $k = 0, \dots, 499$. Since X_{k+1} is a scalar, so is its transpose. Now for the k^{th} data point in each window and for each of the channel i , the iteration is as follows,

For $k = 0$ and $i = 1$,

$$\begin{aligned} [X_1^1] &= \begin{bmatrix} X_0 \end{bmatrix} \begin{bmatrix} a_1 \end{bmatrix} \\ [X_2^1] &= \begin{bmatrix} X_1 \end{bmatrix} \begin{bmatrix} a_1 \end{bmatrix} \\ [X_3^1] &= \begin{bmatrix} X_2 \end{bmatrix} \begin{bmatrix} a_1 \end{bmatrix} \\ &\vdots \\ [X_{500}^1] &= \begin{bmatrix} X_{499} \end{bmatrix} \begin{bmatrix} a_1 \end{bmatrix} \end{aligned}$$

Therefore, (in general) it can be written as,

$$\begin{bmatrix} X_1^1 \\ X_2^1 \\ \vdots \\ X_{500}^1 \end{bmatrix}_{500 \times 1} = \begin{bmatrix} X_0 \\ X_1 \\ \vdots \\ X_{499} \end{bmatrix}_{500 \times 128} \begin{bmatrix} a_1 \end{bmatrix}_{128 \times 1} \quad (3-5)$$

(and so on for a_i for all $i = 1 \dots 128$)

where a_1 is the first row of the \mathbf{A} matrix of a temporal window. Equation 3-5 is of the form $X_{k+1}^1 = X_k * a_1$. From this the least squares problem can be written as,

$$\min_{a_i} \|X_k a_i - X_{k+1}^i\|_2^2 \quad (3-6)$$

Since LASSO is an extension of the least squares problem in Equation 3-6, with the regularisation parameter, this can be modified as,

$$\min_{a_i} \|X_k a_i - X_{k+1}^i\|_2^2 + \beta \|a_i\|_1 \quad (3-7)$$

for all $k = 0, \dots, 499$ and $i = 0, \dots, 128$, where a_i is the i^{th} row of the \mathbf{A} matrix. This way all the rows of the \mathbf{A} matrix is minimised, for all the windows. Equation 3-7 is solved in MATLAB using `cvx` which is a modelling system for solving convex optimization problems efficiently. Since the LASSO problem utilizes L1 norm, `cvx` helps to solve the norm minimization. Appendix C gives more information about the `cvx` and its advantages.

Choosing the tuning parameter β

The crucial part in implementation of LASSO regularisation is the choice of right value for β . The β value aims to make the model sparse in a regularised way to yield a lower prediction error [48]. Choosing this tuning parameter is difficult, as an optimal value needs to be chosen for the lower prediction error. The performance of LASSO depends on choosing the optimal β . For predicting the value of β , one-step ahead prediction error of the obtained model from LASSO for each of the β value is computed. The β with the lowest error is chosen as the optimal value. This is repeated for each of the window for the entire time series.

When the value of $\beta = 0$ in Equation 3-7, the LASSO model formulates as linear regression. Thus, it is useful when the proposed model performance needs to be compared against the linear regression model.

cvx algorithm

The following algorithm was implemented in MATLAB using `cvx` tool.

Algorithm 1 Algorithm for `cvx` to implement LASSO

Require: $\beta \geq 0$

Ensure: window size = 500

$\beta \leftarrow$ desired range of values

$N \leftarrow$ length of β values

$P \leftarrow$ length of total windows

for $n \leftarrow 1$ to N **do**

for $p \leftarrow 1$ to P **do**

for $i \leftarrow 1$ to 128 **do** ▷ number of channels

$a_i \leftarrow p^{th}(i, :)$

`cvx_begin`

variable a_i

$\beta \leftarrow$ variable n

$X_k \leftarrow i^{th}$ data

$X_{k+1} \leftarrow$ one step ahead predicted data

minimize $a_i = \|X_k * a_i - X_{k+1}\|_2^2 + \beta * \|a_i\|_1$

`cvx_end`

end for

end for

end for

3-4 Eigendecomposition

The significant advantage of using the penalized linear approximation is that the dynamics of the brain can be analysed locally by using the eigendecomposition of the obtained state matrix estimates [4]. The \mathbf{A} matrix obtained from the LASSO model for a window by choosing the optimal tuning parameter β , the eigenvalue-eigenvector (eigenmodes) pairs were calculated

for each of the segmented temporal windows. Equation 3-8 gives the decomposition of the state matrix into eigenmodes.

$$x_{k+1} = \mathbf{A}^\top X_k = V\lambda V^\top x_k \quad (3-8)$$

where λ is the eigenvalue and V is the eigenvector. Therefore $p_i(k) = v_i^\top(k)$ gives the i^{th} eigenvector of the i^{th} eigenvalue of the \mathbf{A} matrix. These eigenmodes capture the linearly independent spatial and temporal aspects of the dynamics. In a spatio-temporal analysis, a eigenvector represents where the activation took place (location of the sensor) and the eigenvalues represents the frequency of oscillation of the dynamics.

K-means clustering approach

To choose the eigenvalue-eigenvector pair to visualise the brain dynamics at the given anesthetic stage, K-means clustering approach is considered. Choosing the number of clusters to analyse the dynamics is crucial. Let us consider below three stability scenarios,

- If $|\lambda_i| < 1$, then $|p_i(k)| \rightarrow 0$ as $t \rightarrow \infty$, then the dynamics is asymptotically stable as it vanishes over time.
- If $|\lambda_i| > 1$, then $|p_i(k)| \rightarrow \infty$ as $t \rightarrow \infty$, then the dynamics is unstable as it explodes over time.
- If $|\lambda_i| = 1$, then $|p_i(k)| \rightarrow 0$ as $t \rightarrow 0$, then the dynamics is stable as it oscillates between stable and unstable regimes over time.

The above three criteria are used to see the time evolution of the eigenvalue - eigenvector pair, by looking at its slow and fast decaying oscillations (See Figure 3-3). This way we can better understand the spatial characteristic of the electrodes that were active during a particular anesthetic stage. Therefore, a cluster size $k = 2$ will give a trade-off between these two oscillatory regimes, to better understand the active electrodes (spatial) at different anesthetic stages. This evolution of eigenvalues over time shows changes in the following:

- frequency represented by the angle of eigenvalues; and
- magnitude which represents the spatial profile of the eigenmodes [4].

Clustering is the process of grouping data of similar types. K-means clustering is an algorithm that divides the data into k clusters, in a way that the clustered data forms a similar group [49]. K-means clustering is an unsupervised learning algorithm, which achieves clustering of different groups without training [50]. Each of the cluster is associated with a centroid. The K-means clustering aims to minimise the sum of squares within the cluster. So the process of dividing the data into k clusters is repeated until the best cluster is found [49].

K-means clustering: finds the best value of the centroid (k -center) from its iterative algorithm and assigns the data to its nearest centroid to seek a local optima.

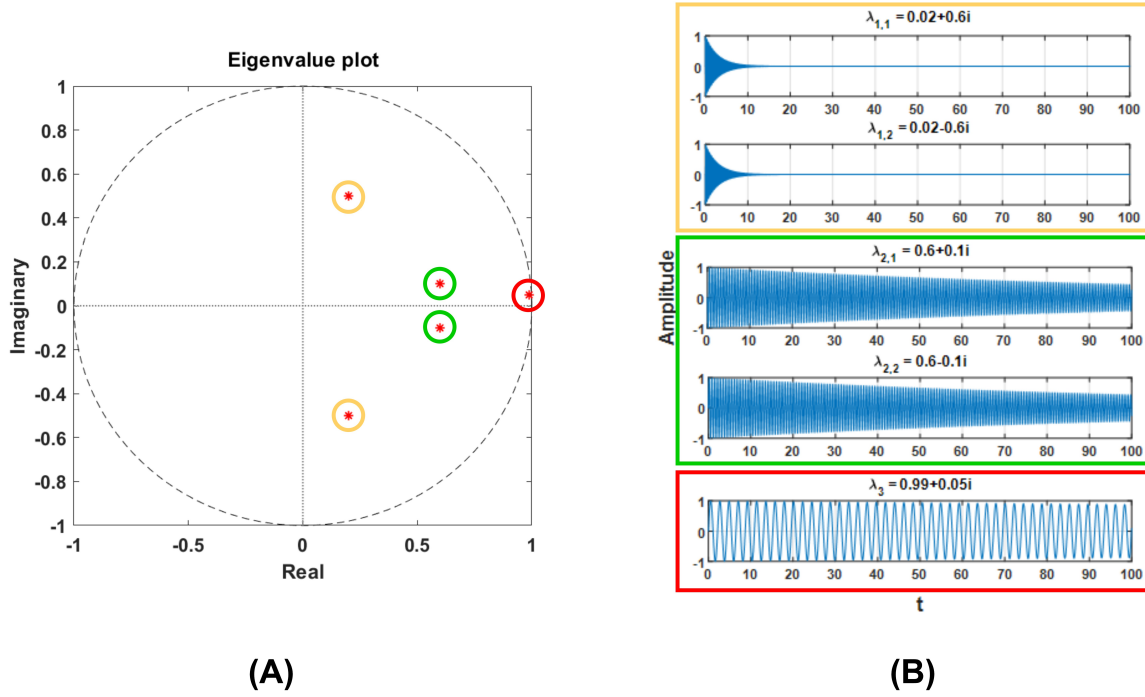


Figure 3-3: Eigenvalue evolution at various stability regimes. (A) shows the plot of example eigenvalues considered whose corresponding evolution (spatiotemporal pattern of oscillations) for the different frequencies are shown in (B) [4].

3-5 Evaluation metrics

The obtained cluster centroids from the K-means clustering can be viewed on the eigenvector plane to see how these cluster points vary between different anesthetic stages. The eigenvalue-eigenvector pair gives the frequency and the direction of oscillation, respectively [4]. The polar coordinates of (λ) are represented as $(\theta_i, |\lambda_i|)$. Thus, the spatial frequency of oscillation from the angle of the eigenvalue can be represented as

$$f_i = \frac{\theta_i}{2\pi} \delta t, \quad (3-9)$$

where δ is the sampling frequency. This spatial frequency depicts slow and fast oscillations. The absolute value of the magnitude of the eigenvalue gives the stability criteria of the ECoG signal at different temporal windows. If the value of the stability is low, then the signal will damp over time to 0. Whereas, when the stability value is higher (i.e., closer to 1) the signals show slow oscillatory behaviour (see Figure 3-3). Hence, having two clusters each one at slow and fast moving oscillatory regimes will give a better intuition on dynamics for the spatio-temporal analysis. The distribution of the frequency and stability at different stages of anesthesia needs to be proven that they are statistically significant (see Appendix D).

3-6 Analysis pipeline

The ECoG data array is split into windows of size 500 ms. Each of these windows is fit into the LASSO regression problem given in Equation 3-7, using `cvx` tool in MATLAB. This is iterated for different values of β and the optimal value is chosen from the one having the lowest one-step prediction error. Then the eigenmodes were calculated for each of the obtained \mathbf{A} matrix for each of the temporal windows. The eigenvectors to be visualised on the brain image is selected based on its spatio-temporal frequency, i.e., the frequency of the corresponding eigenvalue [4], by using K-means clustering. This way the chosen eigenvector gives the direction of the spatiotemporal frequency. For visualising in the brain montage, the eigenvector to be plotted is normalised by dividing each value by the maximum value across its entries. Therefore, we could able to see the evolution spatiotemporal frequency contributed by each of the ECoG channels during different stages of anesthesia. Figure 3-4 explains the process outline.

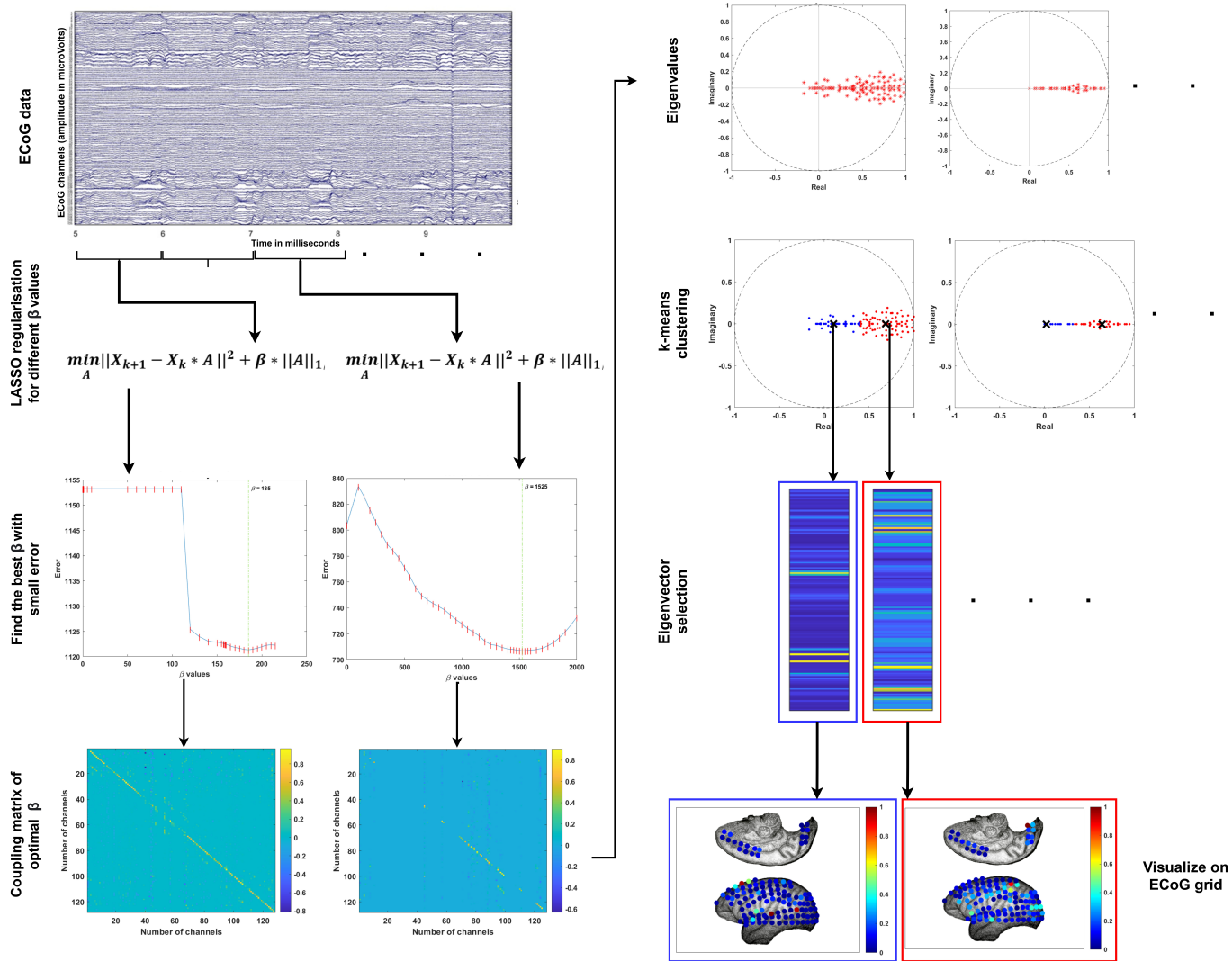


Figure 3-4: Analysis pipeline of the proposed methodology.

Results and discussion

This chapter provides and interprets the obtained results from the proposed model explained in Chapter 3. The modelling methodology was implemented in MATLAB®(9.7, R2019b). The available ECoG data is already pre-processed so it was used directly for analysis. For the implementation of `cvx` for finding an optimal solution, the standard MATLAB `cvx` tool was used. This chapter also addresses the research questions in Chapter 1 and provides claims to support the obtained results in the discussion section. The results are provided for the different stages of anesthesia such that the reader knows how the evolution of dynamics is affected by the induction of anesthesia.

4-1 Estimating state matrix (coupling matrix) from the LASSO model

The ECoG data matrix is split into windows of size 500 ms and the rows of the data is 128, representing the number of channels (electrodes). For ease of understanding, the results for one monkey M2 (see Figure 3-2), induced with anesthetic drug propofol is discussed in the following sections.

The data of monkey M2 induced with propofol drug is provided with 5 different anesthetic stages: anesthesia injected, anesthesia start, anesthesia end, recovery start and recovery end. So, the windows of size 500 ms in spread across all of these stages. The time series is of length 3680698 ms and hence the number of windows of size 500 ms is 7360 . The non-linear dynamics of the brain in each of the windows is linearized using the LTI model proposed in [4], [51].

The linearized matrices need to be simplified by inducing sparsity to capture the spatial temporal aspects of the dynamics. For inducing the sparsity in those matrices, the LASSO modelling formulated in Equation 3-7 is implemented using `cvx` (see Algorithm 1). Equation 3-7 which describes the definition of LASSO.

4-2 Choosing the tuning parameter β

In the cvx algorithm, different β values are used. This way one-step ahead prediction error is performed as the cross validation for choosing the right tuning parameter i.e., optimal β (see Equation 3-7). The obtained state matrices for different β values are used to find the one-step ahead predicted value. This is compared with the original ECoG data point and their error values are calculated. Figure 4-1 shows the error values plotted for different β values for each of the anesthetic stages.

The Table 4-1 gives the β values and their corresponding error values for different stages. The eigendecomposition is performed on these state matrices of chosen β values. For monkey M2, the optimal β values for the anesthetic stages were found to be – see Table 4-1.

Stage	Window number	β value
Anesthesia injected	200	185
Anesthesia start	1500	1500
Anesthesia end	2500	1525
Recovery start	6000	1525
Recovery end	7360	20.5

Table 4-1: Optimal β values obtained for respective temporal windows for different stages of anesthesia.

From Figure 4-1, it can be seen that for $\beta = 0$, which corresponds to the least squares estimate, the error value is higher than the value of optimal β chosen for analysis – see Table 4-2. This way LASSO reduces the model error than the least squares by using the tuning parameter β . So, it is essential that we choose an optimal value of β with minimal one-step ahead error. Also, it is to be noted from Table 4-1 that for each of the windows, the value of β is different that correspond to lowest error. This implies that the model prevents overfitting by optimally tuning the β parameter, thus resulting in a regularised sparsity in the state matrices.

Stage	Error value	
	$\beta = 0$	optimal β
Anesthesia injected	1153.290	1121.376
Anesthesia start	1344.979	1265.100
Anesthesia end	804.267	706.984
Recovery start	1395.716	1313.595
Recovery end	983.351	977.413

Table 4-2: Error values for $\beta = 0$ (least squares) and optimal β for each stage of anesthesia for monkey M2.

The state matrices of the temporal windows at each anesthetic stage with the computed optimal β value is shown in Figure 4-2.

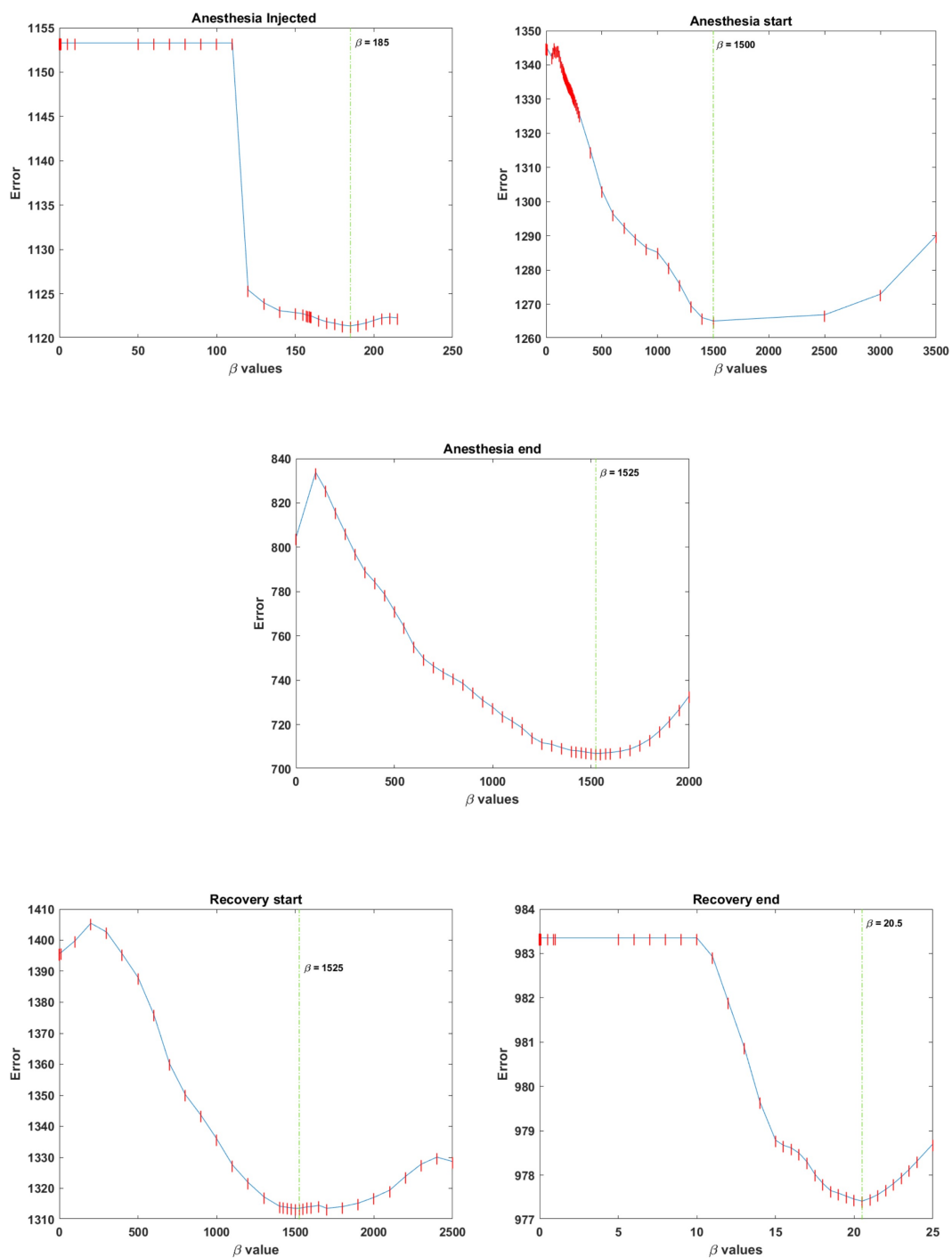


Figure 4-1: One-step ahead error plot for different β values in each window for every anesthetic stage of monkey M2. The green line shows the optimal β value chosen for each of the windows considered. The optimal β corresponding to the green line is mentioned. The red markers show the β value of the computed error.

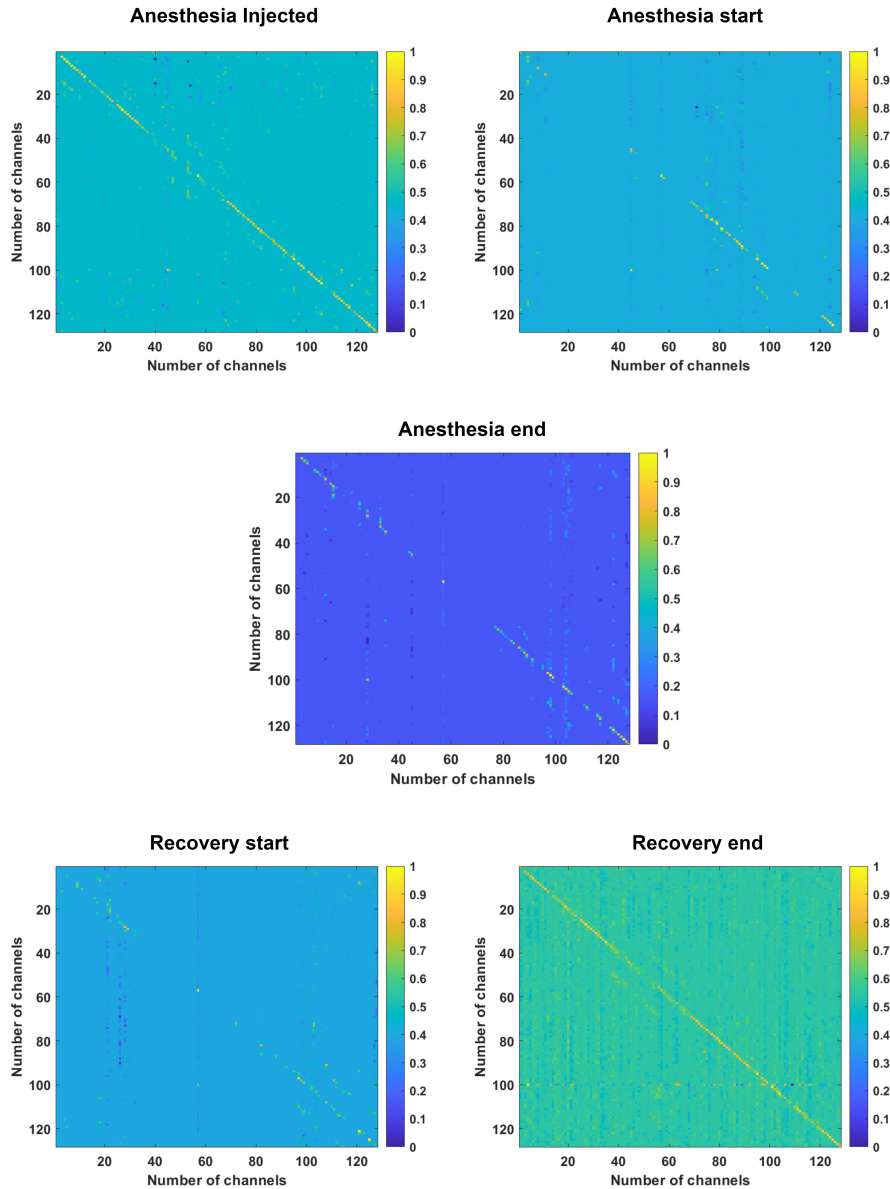


Figure 4-2: State matrices for each of the anesthetic stages (*anesthesia injected, anesthesia start, anesthesia end, recovery start, recovery end*) corresponding to the optimal β value in Table 4-2. The x- and y-axis corresponds to the number of channels (128) implanted in monkey M2.

4-3 Eigendecomposition

The eigenvalues of the state matrices with optimal β value for each stage of anesthesia can be visualised on a complex plane. Figure 4-3 shows the eigenvalue evolution through different anesthetic stages.

From Figure 4-3, it can be noticed that, as the subject enters to anesthetic start stage eigenvalues shrinks in complex magnitude and converge towards the real axis. During the injection and recovery stage the eigenvalues are spread in the complex plane. This criteria is easier to

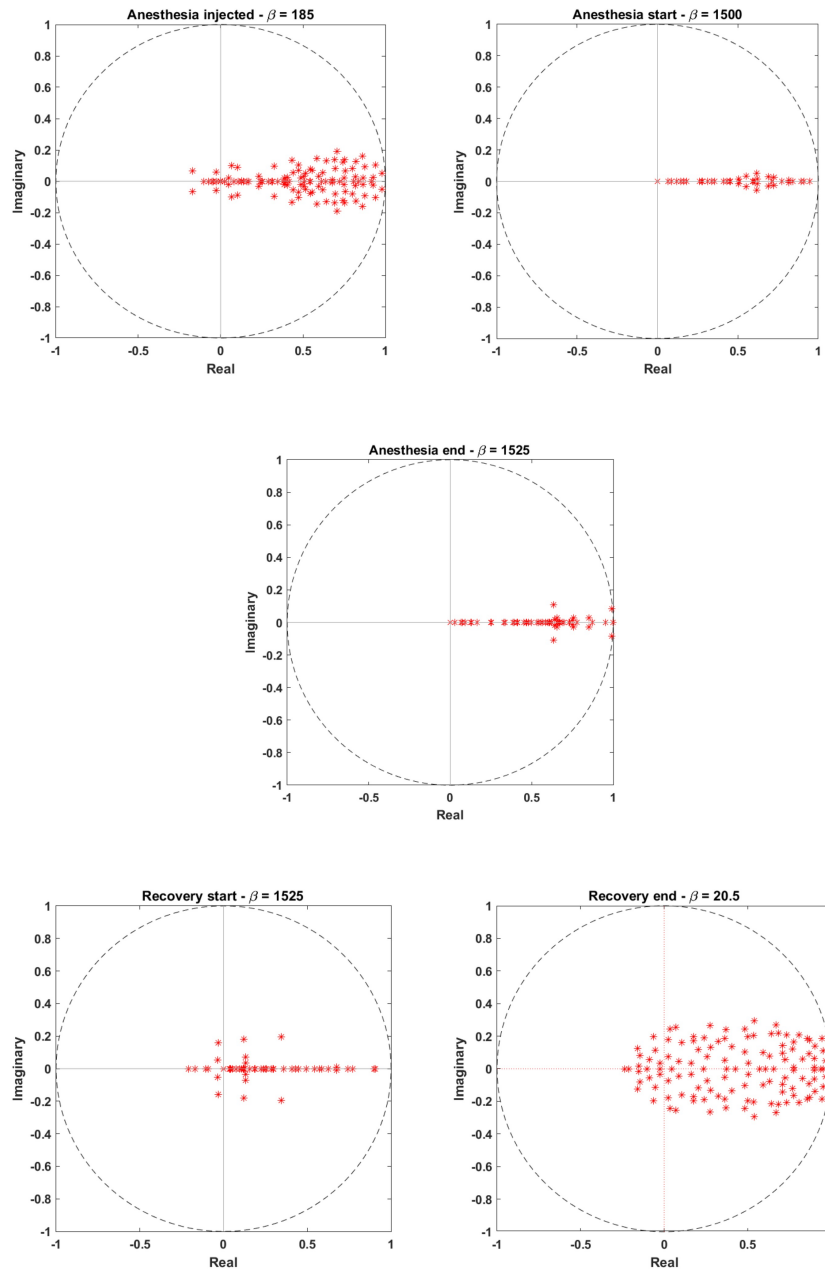


Figure 4-3: Eigenvalues for the state matrices for β values in Table 4-1 for each of the anesthetic stage.

interpret to say if the anesthesia stage has started, rather than dynamical stability method in [5], using criticality index.

The changes in dynamics of the local oscillation which accounts for the spatiotemporal evolution is effectively captured from the eigenmodes. Since there are 128 channels, it is crucial to choose one channel that contributes to the dynamics the most without the expense of dropping another channel that contributes to the spatiotemporal evolution. For choosing the appropriate eigenvector, a classification is done with the eigenvalues. In this thesis, K-means

clustering (see Section 3-4) is utilised to choose the eigenvalues and find its corresponding eigenvectors to visualise on the monkey brain montage. The cluster size chosen is 2, as explained in Section 3-4, two clusters can give two centroids on the complex plane such that there is a trade-off between the slow and fast decaying oscillations. Figure 4-4 shows the centroids obtained from K-means clustering.

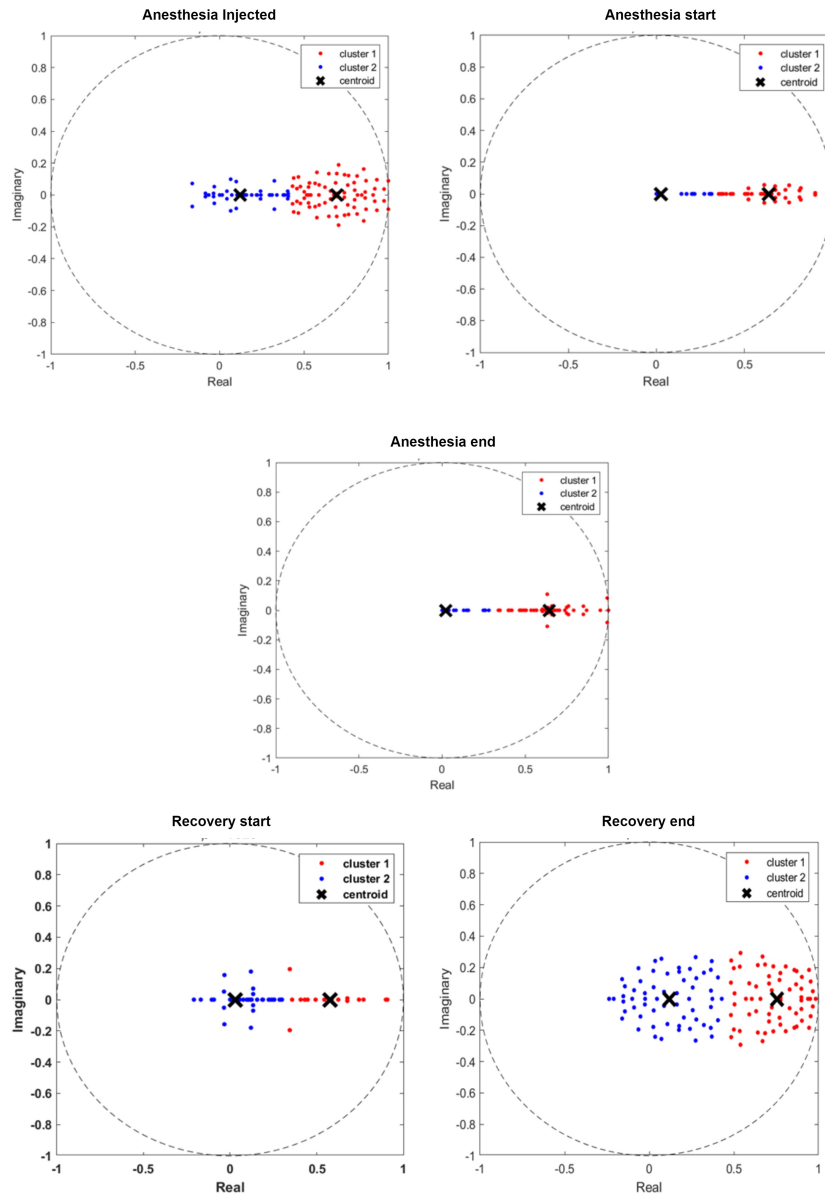


Figure 4-4: K-means clusters of eigenvalues in Figure 4-3 for windows given in Table 4-1 in each of the anesthetic stages. The red clusters correspond to cluster 1 representing fast wave oscillations and the blue clusters correspond to cluster 2 representing slow wave oscillations. The x mark represents the centroids of each of the clusters.

From Figure 4-4, the eigenvalues in blue clusters correspond to slow decaying oscillations whereas the eigenvalues in red clusters correspond to fast decaying oscillations. Furthermore, the frequency vs. stability plot of the eigenvalues for different anesthetic stages are shown in

Figure 4-5. Visually it can be seen that the eigenvalue cluster distributions are not similar between the different stages. To prove that the clusters are statistically different, two-sample Kolmogorov-Smirnov (K-S) test is carried out (see Appendix D). The test rejects the null hypothesis that the distribution of eigenvalue clusters between different anesthetic stages are statistically similar, at a significance level of 5%.

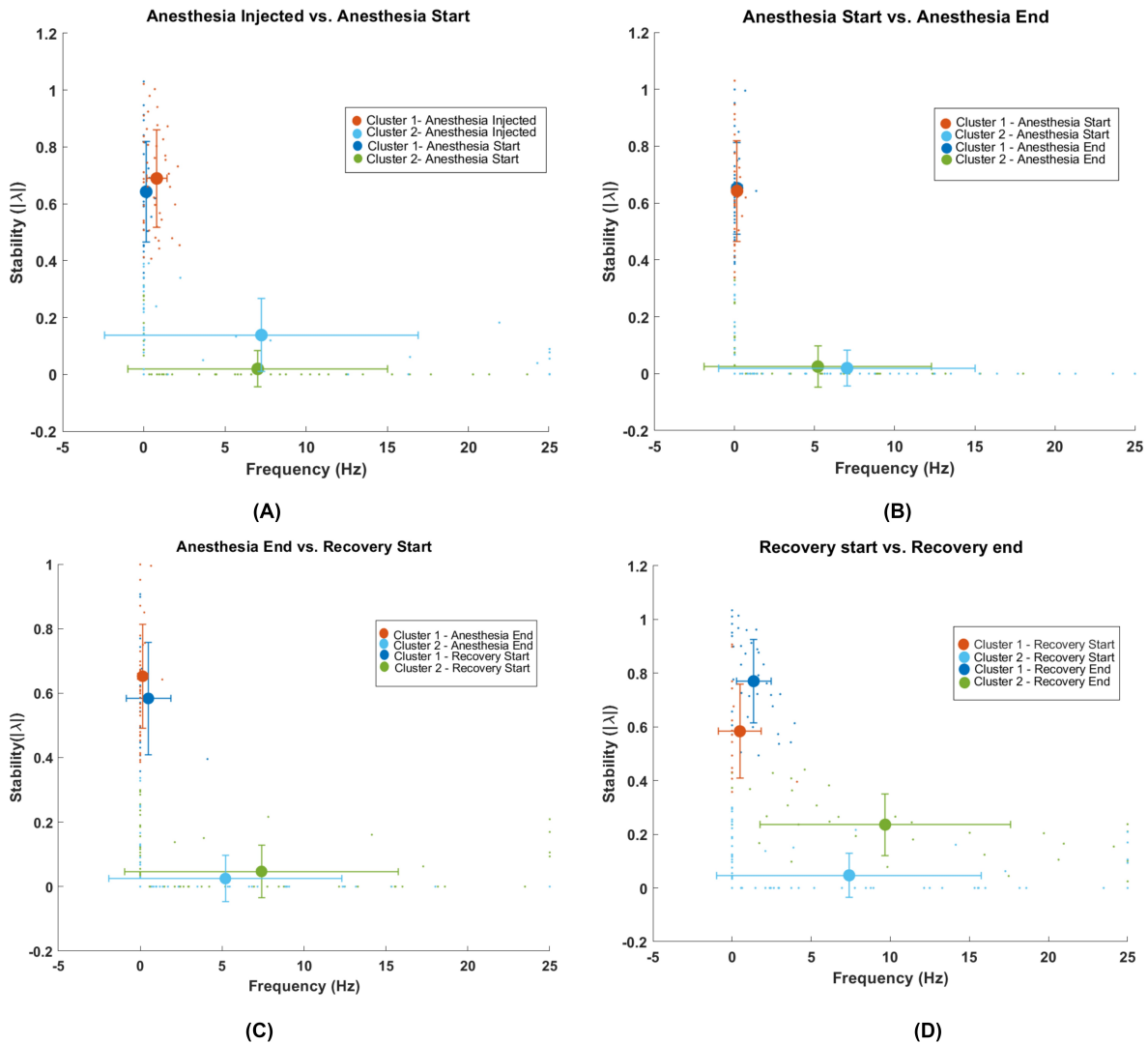


Figure 4-5: Spectral clustering of the eigenvalues of state matrices resulted from the LASSO model based on the frequency and stability (argument and absolute magnitude respectively) of eigenvalue. The coloured dots represent the distribution of eigenvalues from the K-means clustering of different anesthetic stages for monkey M2 with propofol drug. Error bar gives the mean and standard deviation from frequency and stability of each of the clusters. Distribution of cluster points is shown for (A) anesthesia injection vs. anesthesia start, (B) anesthesia start vs. anesthesia end, (C) anesthesia end vs. recovery start, (D) recovery start vs. recovery end.

The eigenvectors of the centroids are visualised on the brain montage of monkey M2 (see Figure 3-2). Figure 4-6 shows the eigenvector of centroids for different stages of anesthesia.

The visualisation on brain montage is compared with the regions of the brain shown in Figure 3-1, to relate the active regions and the stage of anesthesia. From Figure 4-6, the following inferences can be obtained for the different stages of anesthesia,

- **Anesthesia injection:** The electrodes near the parietal lobe and occipital lobe shows some oscillatory values. During this stage, the subject might have experienced some pain and was awakened, which could account for these oscillations.
- **Anesthesia start:** Not much oscillations could be observed near the frontal cortex and also in the visual cortex. This can be interpreted as the subject to have entered into the anesthetic stage.
- **Anesthesia end:** Same as anesthesia start, anesthesia end also shows oscillations in one or two electrodes. Anesthesia end however means that the anesthetic dosage was stopped, yet the subject has not recovered from unconsciousness.
- **Recovery start:** The brain visualisation clearly shows some oscillation in the audio and visual cortex, which clearly says the subject is recovering from anesthesia.
- **Recovery end:** Many oscillatory electrodes in the regions of the brain are observed here, which clearly justifies that the subject has recovered from its unconscious state.

The results above clearly show that the electrodes rightly interprets the anesthetic stages and that the model has rightly captured the dynamics of the brain. The results from ECoG data for other monkeys (M1, M3, and M4) are presented below.

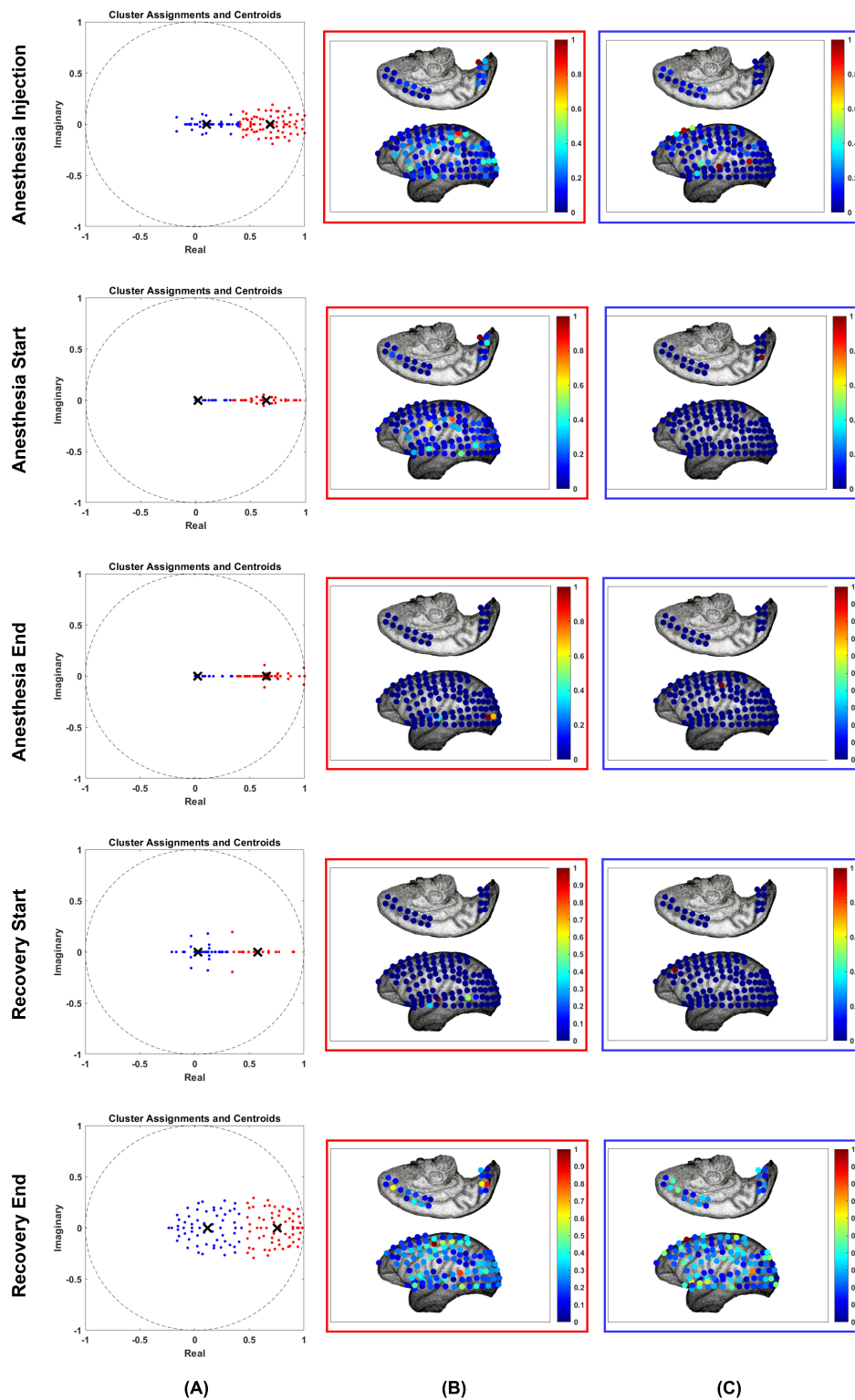


Figure 4-6: Eigenvector of the centroids from K-means clustering for different stages of anesthesia - Monkey M2 with propofol. (A) shows the eigenvalue distribution with 2 clusters (red - cluster1 and blue - cluster2) from K-means clustering, (B) eigenvector of centroid of cluster 1, (C) eigenvector of centroid of cluster 2, visualised on electrode configuration. The colorbar in (B) and (C) represents the normalised eigenvector values.

Results for monkey M1 with drug propofol

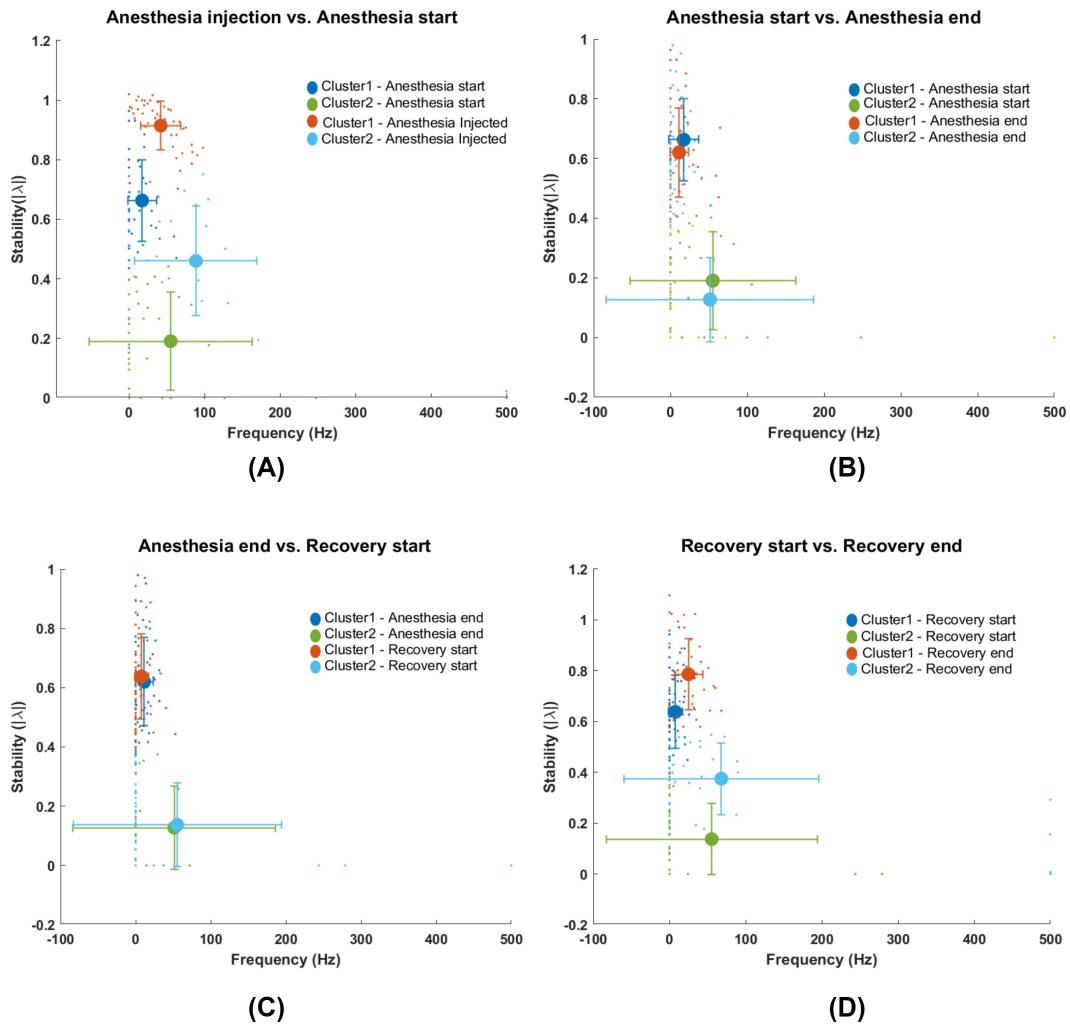


Figure 4-7: Spectral clustering of the eigenvalues of state matrices resulting from LASSO model based on the frequency and stability (argument and absolute magnitude respectively) of eigenvalue. The coloured dots represent the distribution of eigenvalues from the K-means clustering of different anesthetic stages for monkey M1 with propofol drug. Error bar gives the mean and standard deviation from frequency and stability of each of the clusters. Distribution of cluster points is shown for (A) anesthesia injection vs. anesthesia start, (B) anesthesia start vs. anesthesia end, (C) anesthesia end vs. recovery start, (D) recovery start vs. recovery end.

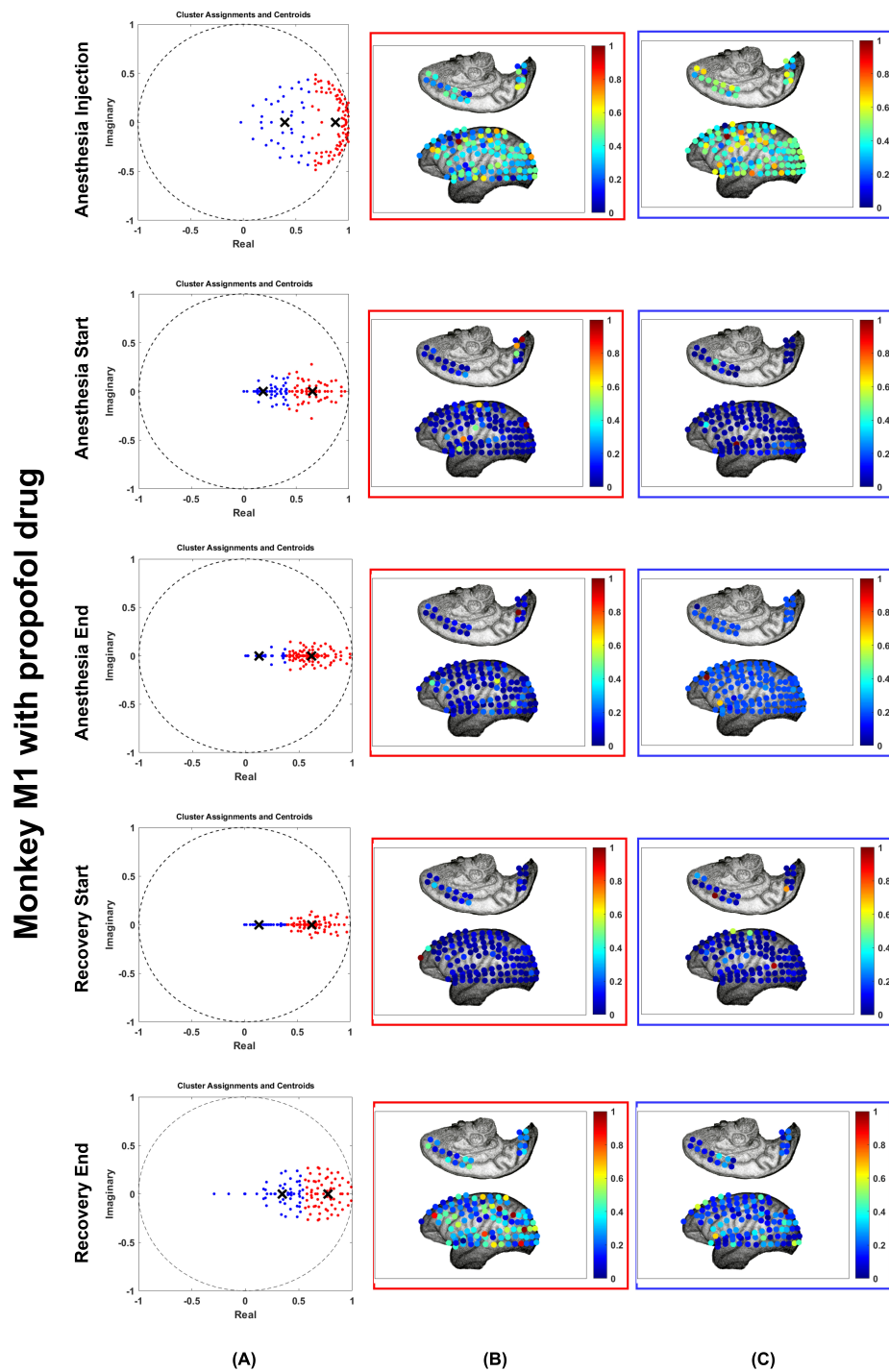


Figure 4-8: Eigenvector of the centroids from K-means clustering for different stages of anesthesia - Monkey M1 with propofol. (A) shows the eigenvalue distribution with 2 clusters (red - cluster1 and blue - cluster2) from K-means clustering, (B) eigenvector of centroid of cluster 1, (C) eigenvector of centroid of cluster 2, visualised on monkey M1 electrode configuration. The colorbar in (B) and (C) represents the normalised eigenvector values.

Reviewing results in Figure 4-7 and Figure 4-8:

- The eigenvalue pattern in Figure 4-8 (A) converges towards the real axis through anesthesia injected and anesthesia end stages and is found to be spreading out during the recovery stage.
- From K-S test, eigenvalue clusters reject the null hypothesis that their distribution in different stages of anesthesia are statistically similar at a significance level of 5%.
- The dynamics captured by the LASSO model which is visually represented in Figure 4-8 (B) and (C) shows the frontal region of the brain (see Figure 3-1 for reference) has very minimal oscillations during anesthetic start to recovery start stage.
- Anesthesia injected and recovery end stages show oscillations in many electrodes than other stages. This indicates that the subject was awakened and active.

Results for monkey M3 with drug ketamine-medetomidine

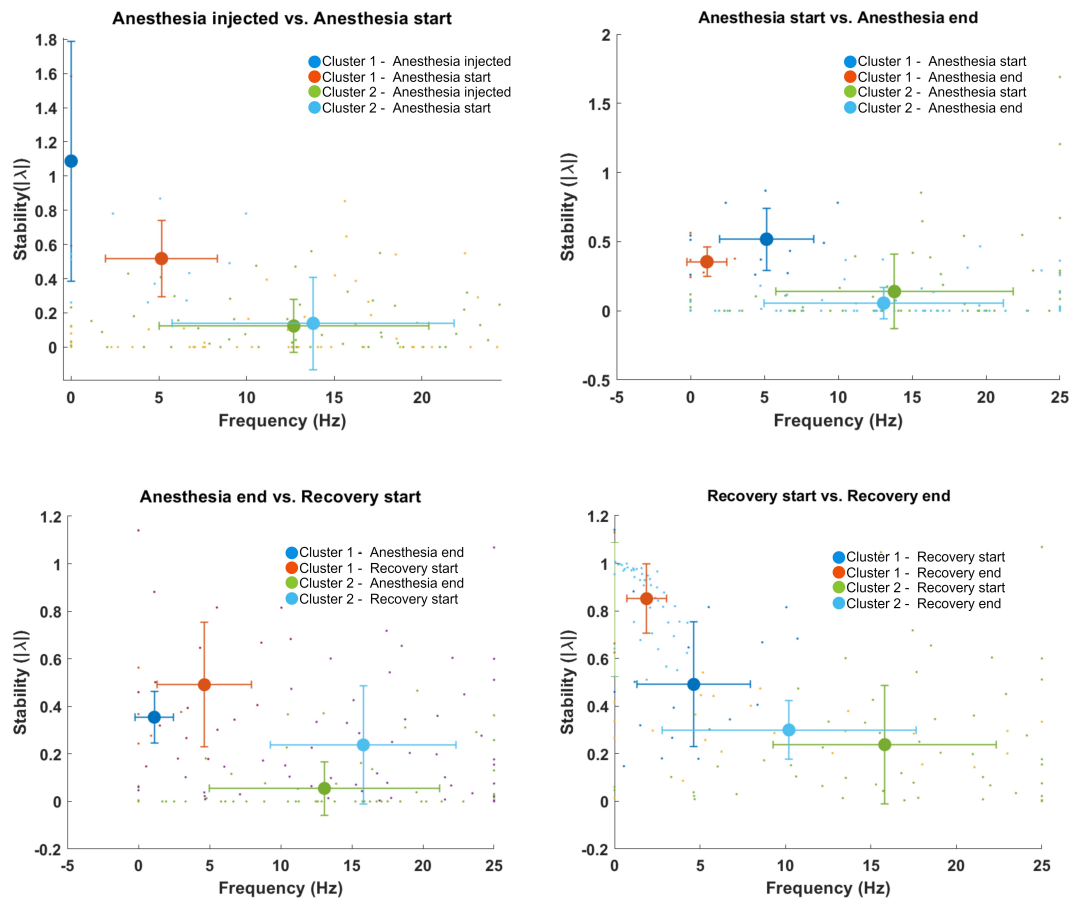


Figure 4-9: Spectral clustering of the eigenvalues of state matrices resulting from LASSO model based on the frequency and stability (argument and absolute magnitude respectively) of eigenvalue. The coloured dots represent the distribution of eigenvalues from the K-means clustering of different anesthetic stages for monkey M3 with ketamine-medetomidine drug. Error bar gives the mean and standard deviation from frequency and stability of each of the clusters. Distribution of cluster points is shown for (A) anesthesia injection vs. anesthesia start, (B) anesthesia start vs. anesthesia end, (C) anesthesia end vs. recovery start, (D) recovery start vs. recovery end.

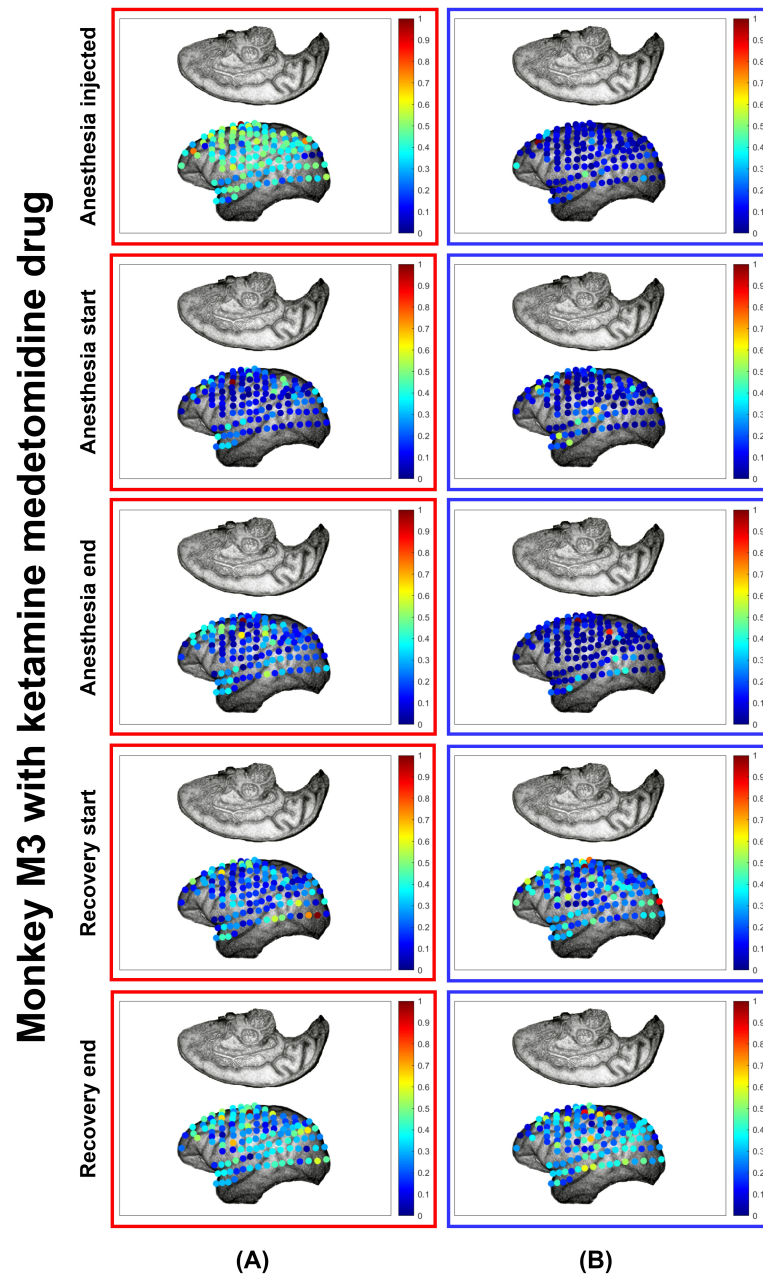


Figure 4-10: Eigenvector of the centroids from K-means clustering for different stages of anesthesia - Monkey M3 with ketamine-medetomidine. (A) shows the eigenvalue distribution with 2 clusters (red - cluster1 and blue - cluster2) from K-means clustering, (B) eigenvector of centroid of cluster 1, (C) eigenvector of centroid of cluster 2, visualised on monkey M3 electrode configuration. The colorbar in (B) and (C) represents the normalised eigenvector values.

Reviewing results in Figure 4-9 and Figure 4-10:

- From Figure 4-9 it can be seen that the clusters (obtained from K-means) between different anesthetic stages under comparison are not identical.
- From K-S test, eigenvalue clusters reject the null hypothesis that their distribution in different stages of anesthesia are statistically similar at a significance level of 5%.
- The dynamics captured by the LASSO model which is visually represented in Figure 4-10 (A) and (B) shows some oscillations in the prefrontal cortex and parietal lobe (see Figure 3-1 for reference) in anesthesia end stage. The subject might have started to recover to a conscious state during that time window.
- Anesthesia injected and recovery end stages show oscillations in many electrodes than other stages. This indicates that the subject was awakened and active.

Results for monkey M4 with drug ketamine-medetomidine

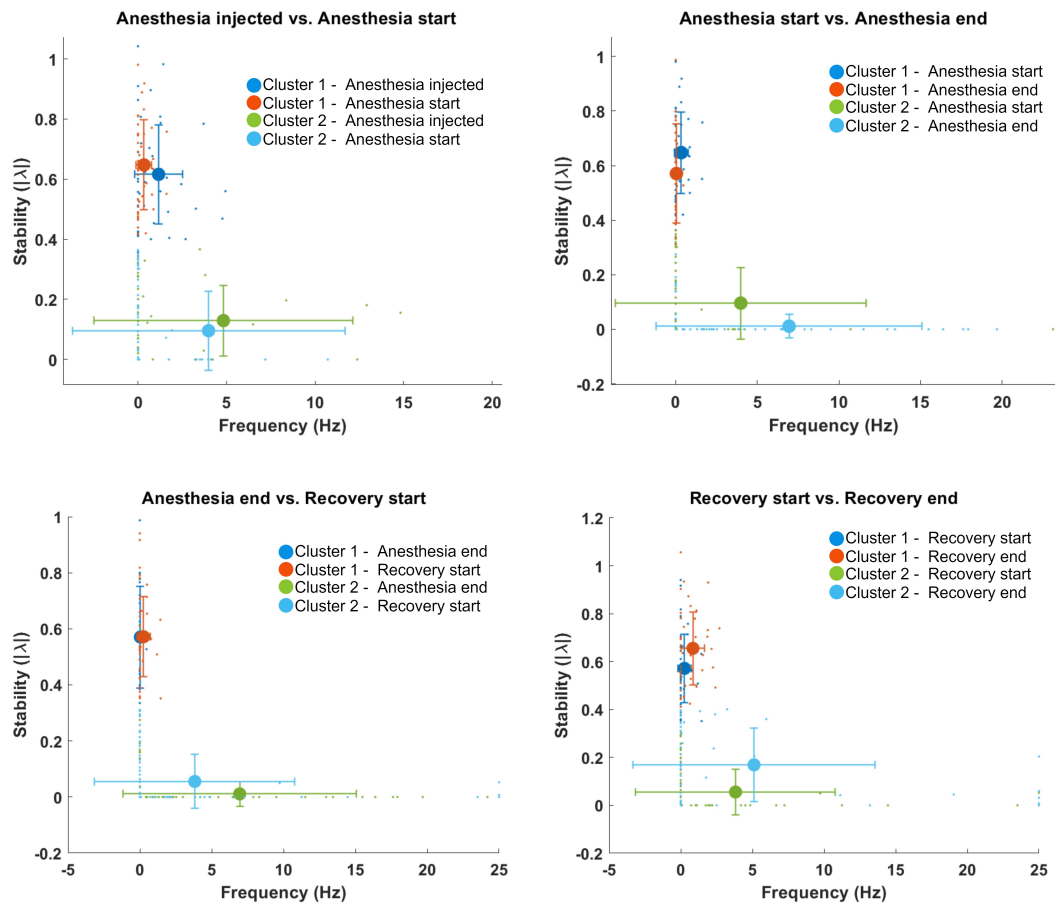


Figure 4-11: Spectral clustering of the eigenvalues of state matrices resulting from the LASSO model based on the frequency and stability (argument and absolute magnitude respectively) of eigenvalue. The coloured dots represent the distribution of eigenvalues from the K-means clustering of different anesthetic stages for monkey M4 with ketamine-medetomidine drug. Error bar gives the mean and standard deviation from frequency and stability of each of the clusters. Distribution of cluster points is shown for (A) anesthesia injection vs. anesthesia start, (B) anesthesia start vs. anesthesia end, (C) anesthesia end vs. recovery start, (D) recovery start vs. recovery end.

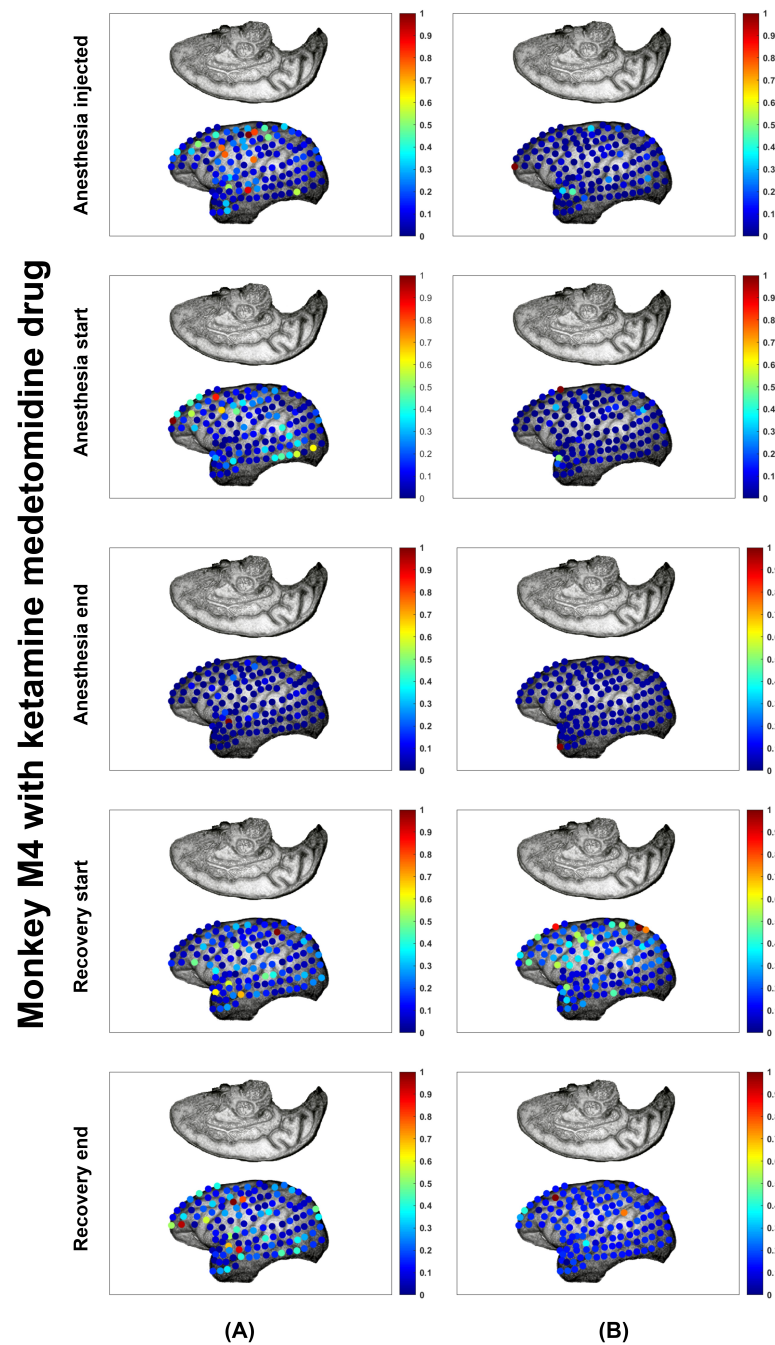


Figure 4-12: Eigenvector of the centroids from K-means clustering for different stages of anesthesia - Monkey M4 with ketamine-medetomidine. (A) shows the eigenvalue distribution with 2 clusters (red - cluster1 and blue - cluster2) from K-means clustering, (B) eigenvector of centroid of cluster 1, (C) eigenvector of centroid of cluster 2, visualised on monkey M4 electrode configuration. The colorbar in (B) and (C) represents the normalised eigenvector values.

Reviewing results in Figure 4-11 and Figure 4-12:

- From Figure 4-11 it can be seen that the clusters (obtained from K-means) between different anesthetic stages under comparison are not identical.
- From K-S test, eigenvalue clusters reject the null hypothesis that their distribution in different stages of anesthesia are statistically similar at a significance level of 5%.
- The dynamics captured by the LASSO model which is visually represented in Figure 4-12 (A) and (B) shows some oscillations in the prefrontal cortex and parietal lobe (see Figure 3-1 for reference) in anesthesia start stage. The subject might be entering an unconscious state and not completely into it yet. This could have contributed to the respective oscillations.
- Anesthesia injected and recovery end stages show oscillations in many electrodes than other stages. This indicates that the subject was awakened and active.

4-4 Discussion

The results provided in the previous sections are discussed in brief addressing the research questions formulated in Chapter 1. This section focuses on a comparative and quantitative analysis of the obtained results, to show the performance of the proposed model.

A regularized method to induce sparsity to capture the dynamics:

The ECoG data analysis is leveraged by using the LASSO model proposed in Equation 3-7, such that the state matrices are induced with sparsity to capture the right dynamics. The method of sparsifying the state matrices done in [5] studies about the stability in loss of consciousness using a threshold criteria. Rather, the LASSO model has regularised the way of sparsification using the tuning parameter β . A sanity check to induce the same amount of sparsity followed in [5] was tuned in the LASSO model to get the same amount of sparsity. It was seen that the LASSO model could capture some oscillation for the anesthesia injected stage, whereas the threshold method was completely flat with values 0 for all the electrodes (see Appendix A-2). This has clearly addressed the RT1 and RT5 in Section 1-2.

Trade off between sparsity of the matrices

The tuning parameter β regularises the sparsity induced in each of the state matrices of the temporal windows. The results were presented for one window in each of the anesthetic stages in Figure 4-5. The other neighbouring windows also showed similar results. A sanity check is shown in Appendix A for monkey M2 in anesthetic start stage for a neighbouring window (window 1501) (see Appendix A-1). The neighbouring window shows similar oscillations justifying that the proposed model rightly captures the dynamics between and within the different anesthetic stages. The tuning parameter β is not the same for every window in the same anesthetic stage. Anesthetic start stage in Figure 4-1 has a optimal β value of 1500 whereas its neighbouring window has a β value of 225. Yet the oscillations contributed from the resulting state matrices have similar behaviour, hence, justifying the subject to belong in anesthetic start stage. The proposed model does ensure that the sparsity of the matrices induced by the tuning parameter β , rightly captures the dynamics of the brain. Thus, RT2 in Section 1-2 has been handled by the proposed LASSO model.

Proposed model vs. overfitting

Overfitting can be one of the major issues while trying to give a better model for studying the dynamics under different anesthetic stages. The proposed model is found to be handling the problem of overfitting with the help of β tuning parameter. Finding the right β with one-step ahead prediction error has addressed the occurrence of over-fitting. A same value of β for the different stages can cause over-fitting or under-fitting (see Appendix B), but this was avoided by finding the one-step ahead error for each of the windows and by customizing the β value. Hence, RT3 in Section 1-2 has been addressed by the proposed LASSO model.

Eigenmode analysis

In the proposed methodology, eigenmode decomposition, i.e., eigenvalue-eigenvector pair was

computed for analysis of the brain dynamics. In the exiting work in literature [5], only the magnitude of the eigenvalues were considered, whereas the proposed method utilizes eigenvectors and the angle of eigenvalue. By choosing the eigenvalues that gives a trade-off between slow and fast decaying oscillations, and visualising their corresponding eigenvectors has given great insights to differentiate between anesthetic stages. The oscillations viewed on the electrode map in Figure 4-6, 4-8, 4-10 and 4-12 rightly relates to the anesthetic stages by comparing it with the brain regions in Figure 3-1 and each of its functional characteristics. This method can hence be a starting point in developing signatures that can identify the stages with real time data, thus addressing the RT5 in Section 1-2.

LASSO model over least squares

The LASSO model in Equation 3-7 is an extension of the least squares model. If the β value in Equation 3-7 is 0, it formulates as least squares minimization problem. But from the Figure 4-1 and Table 4-2, it can be clearly seen that the error from one-step ahead prediction is high for $\beta = 0$ than the chosen optimal β value. Perhaps, β , the tuning parameter present in LASSO is an advantage over the least squares technique.

Advantages of the proposed methodology

- The proposed model uses the tuning parameter β to regularise the sparsity of the system matrices. Since each of the temporal windows are computed for its optimal β value, the analysis of the brain dynamics is improved under anesthesia.
- The performance of proposed model is not influenced by the type of drug induced to the patient/subject. Present day anesthesia monitors, however, do not perform well under certain types of anesthetic drugs. Since the type of drug is not the parameter of interest while modelling, it does not have a greater effect on the results.
- The end results, i.e., the electrode oscillations obtained from the eigenvectors are visualised on the brain montage with electrode configuration of the patient. This enhances the output interpretation in real time rather than an index value used in present day DoA monitors.
- The data used for analysis was from ECoG, whereas EEG is a commonly used imaging technique. Since EEG is a non-invasive method to capture the brain waves, the skull of the head can act as a high pass filter. Therefore, only fast decaying oscillations could be captured. But with the help of ECoG data, it was possible to study and analyse using both fast and slow decaying oscillations.

Chapter 5

Conclusion

Unconsciousness caused by induction of general anesthesia has no reliable method to be distinguished from awake or unconscious state, with respect to brain activity [10]. The distinguishing property between conscious and unconscious states is still unknown and is highly in debate question in the field of neuroscience. Despite anesthesiologists having experience with awareness and about amount the of anesthetic induction to be dosed, the procedure to find if the patient might recover from unconsciousness still remains imperfect. In this thesis, a control theoretic approach was derived to quote the different stages of anesthesia from ECoG data collected from patients. The results discern a pattern of behaviour from the eigendecomposition, which can be viewed on the brain map, leveraging the method of monitoring the anesthetic stages in patients.

The existing methods in literature suggested that stability plays an important role in defining consciousness. The proposed methodology in Chapter 3, is a cut above approach to stability analysis that studies the properties of the dynamical system. Results in this thesis have improved the assessment of the brain anesthetic states, by inducing a regularised way to choose the right parameters that contribute to the dynamics. Sections 4-2 and 4-3, highlight how the proposed model was designed to choose the tuning parameter that captures the system dynamics and how those dynamics can be viewed to distinguish between different anesthetic stages. However, from the eigendecomposition, choosing the right eigenvalue to visualise the eigenvector was a challenge. It was solved by using K-means clustering, of cluster size 2, which gives a trade-off between slow/fast decaying oscillations highlighted in Figure 4-6.

The minimization problem implemented in `cvx`, which formulates as a convex optimization problem, and to find the minimum with β (in Equation 3-7) having different values. Specifically, the proposed model aims to pinpoint the regions of the brain that were active during different anesthetic stages. This was achieved through the eigenvectors, that were visualised on the brain electrode mapping. Therefore, it highly helps the end user to clearly have an idea of the change in dynamics of the brain through the different anesthetic changes. Section 4-3 highlight how electrode activity minimized during the active anesthetic stages, which also can

be seen in the pattern of eigenvalue evolution (see Figure 4-6). To validate and support the claims that address the research questions, various sanity checks were done, whose results are attached in the Appendix A. Overall, the proposed methodology paves a way for a high level method of anesthetic stage signatures, which can improve the monitoring of patients (physiologically they are similar to primates) induced with similar anesthetic drugs explored in this thesis.

5-1 Limitations

The proposed method was worked with ECoG data. It is not the most commonly used clinical medical imaging technique. As ECoG is an invasive technique, it is limited to a specific group of patients, for example, with epilepsy. While electroencephalograph (EEG) is the widely used imaging technique for capturing the brain. It is also easy to mount to the head of the patient as the electrodes are fitted to a cap shape structure and work by the patient (non-invasive). The EEG data is prone to artefacts and the number of electrodes covering the head surface is lesser compared to ECoG. The proposed model may have to be effected with minor changes to mitigate the characteristics of EEG. The performance of the proposed model with EEG data is unknown as the gel patch used to stick the electrodes of EEG, the skull surface of the head and the number of electrodes in EEG might affect.

The proposed model was tested on a laptop with limited processor specifications. Hence the speed of computation was long and therefore to get the results without delay with real time data a processor with high speed may be required.

5-2 Future work

This research work uses ECoG data from monkeys. While EEG is the most commonly used and the easiest method to capture brain signals, the performance of the proposed methodology can be tested with EEG data from humans. The structure and function of the human brain is more or less the same as that of monkeys. Therefore, the study of comparison using active electrodes on the regions of the brain, during different anesthetic stages should not affect (see page 34). Unlike the ECoG, which are implanted into patients per specific regions of purpose, the EEG electrodes have a standard configuration, hence, the electrode mapping to view the active electrodes will be the same for all patients.

The proposed methodology can also be implemented in future in a robotic surgery environment, where the anesthesia can be monitored by viewing the changed in the electrode mapping and induce anesthetic drugs when needed. But this shall be a phase after rigorous tests and validations had been carried out on multiple levels, such that the model gains the confidence among the anesthesiologists and doctors.

Appendix A

Sanity checks

The LASSO model proposed needs to clear few sanity checks to prove its authenticity. This section provides results on some of the criteria that the writer anticipates as potential queries among the readers.

A-1 Sanity check with neighbouring windows

The results shown in the Section 4-3 were for only one of the windows in each of the anesthetic stage. The model has to perform and provide the same results for the neighbouring windows of the same anesthetic stage. Figure A-1 shows the results of window 1501 (in Section 4-3, result was provided for window 1500), which corresponds to the anesthesia start stage. From Figure A-1, it can be seen that the results are similar that was presented in Figure 4-6 for anesthesia start stage (window 1500)

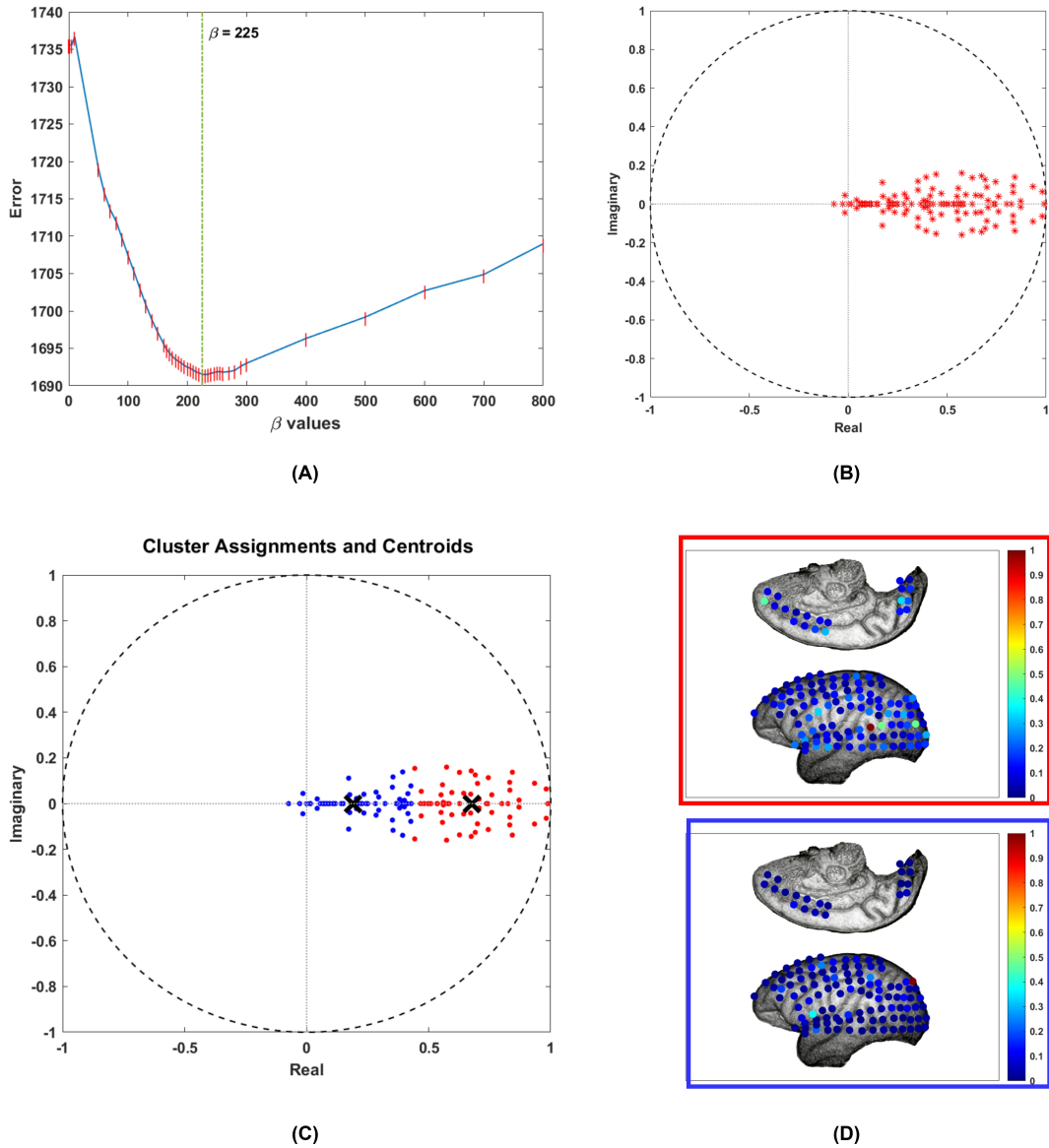


Figure A-1: Result for Monkey M2 induced with propofol in anesthesia start stage (window 1501). (A) shows the one-step ahead error plot for β values, with optimal beta β shown with green vertical line. (B) shows the eigenvalue plot from the state matrix of the chosen β in a complex plane. (C) shows the cluster assignments and centroids from K-means clustering and (D) shows the eigenvector plot of the centroids in (C) on monkey M2 electrode configuration.

A-2 Sanity check with same amount of sparsity

The sparsity induced in [5] is by using the threshold criteria. The number of zeros for one of the window is checked and the same amount of sparsity is induced in the LASSO model for the same window by tuning the β parameter. Figure A-2 shows the window corresponding to anesthesia start for same number of zeros for both the threshold criteria and LASSO method.

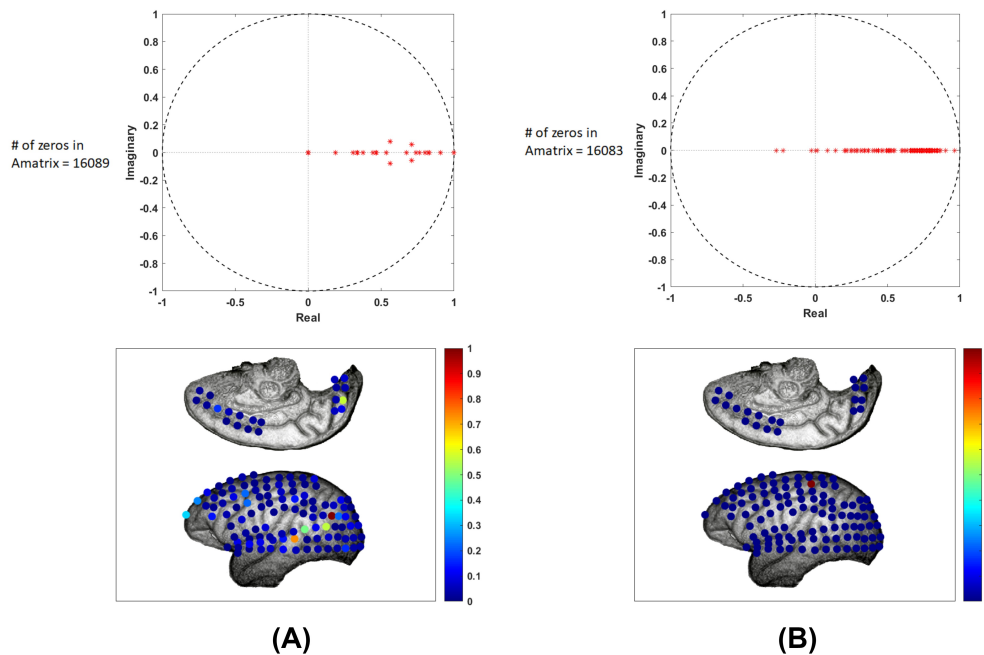


Figure A-2: Plots showing the results with same amount of sparsity induced in LASSO model in Equation 3-7 and from threshold criteria in [5]. (A) shows the eigenvalue (top) and eigenvector plot (bottom) from LASSO model which is tuned using the β parameter to have same amount of sparsity obtained through threshold criteria shown in (B) (top - eigenvalue plot, bottom - eigenvector plot)

LASSO has captured some dynamics even with the same sparsity criteria used. It can be argued that the feature selection by LASSO captures the right dynamics without dropping it.

Appendix B

Supplementary

B-1 Effect of same β values

In the proposed model LASSO allows to tune the β parameter for each of the temporal windows to get the sparsification of the state matrices. The following results shows the effect of β being the same value (> 0), and analyse how it affects the visualisation of the dynamics.

It can be noted from Figure B-1 that the dynamics for anesthesia injected, recovery start and recovery end is different from that was obtained for different β values through one-step ahead error in Figure 4-8. Since the β value was fixed, it has greatly affected the dynamics being visualised. It can be difficult to differentiate between the stages as they more or less look similar (see Figure B-1 (A) and (B)). Therefore, finding the optimal β value for each of the temporal windows can be preferred, than having same value of β for all the windows.

Monkey M1 with propofol for $\beta = 1000$

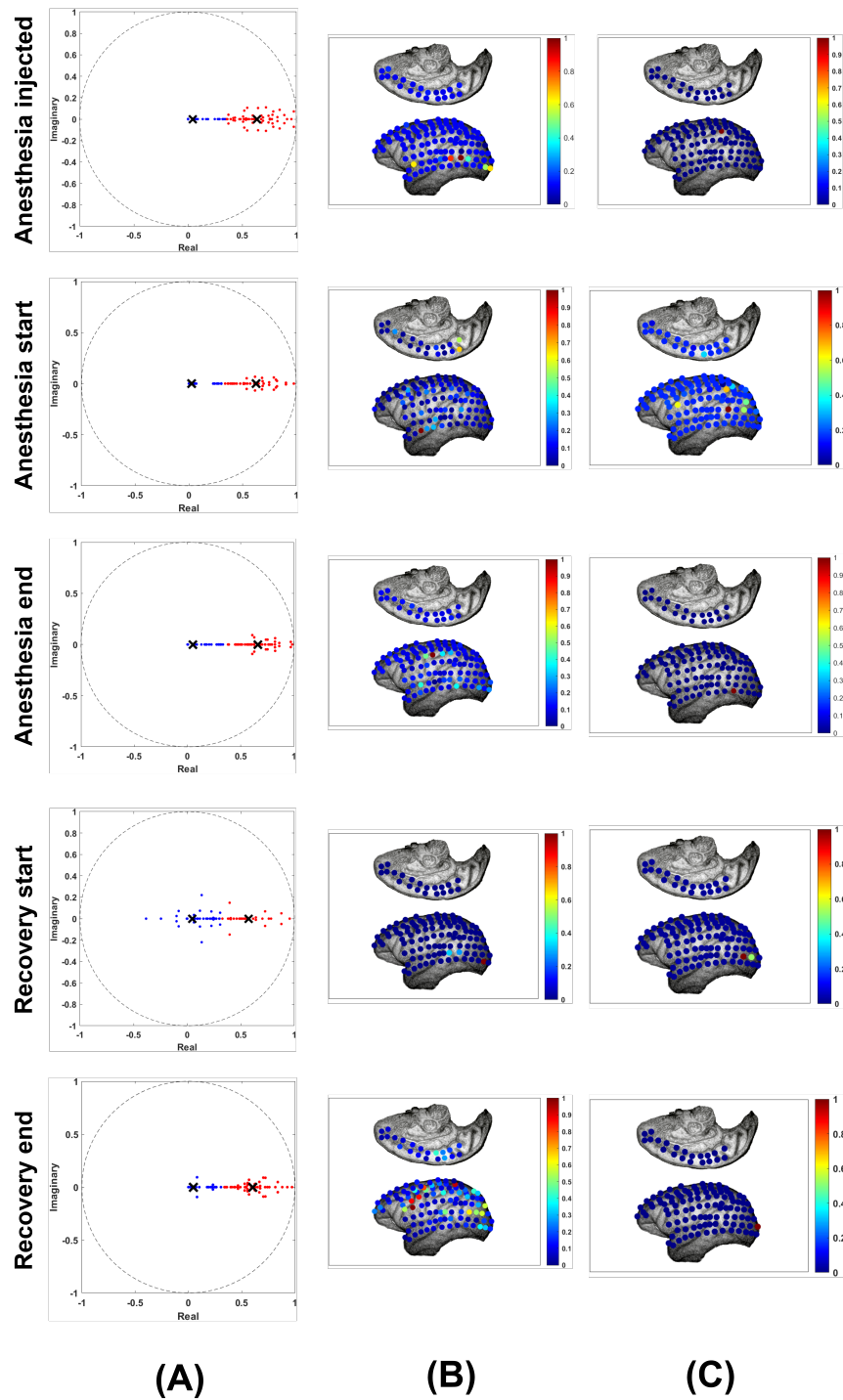


Figure B-1: Eigenvector of the centroids from K-means clustering for different stages of anesthesia - Monkey M1 with propofol for $\beta = 1000$. (A) shows the eigenvalue distribution with 2 clusters (red - cluster1 and blue - cluster2) from K-means clustering, (B) eigenvector of centroid of cluster 1, (C) eigenvector of centroid of cluster 2, visualised on electrode configuration. The colorbar in (B) and (C) represents the normalised eigenvector values.

Appendix C

About `cvx`

`cvx` is a MATLAB modelling tool to solve convex optimization problem. In general, it is used to solve linear programs, quadratic programs and also l_1 norms. `cvx` tool enables to formulate and solve minimization, maximization and other problems. In the proposed methodology, the LASSO model in Equation 3-7, was implemented using `cvx`. The algorithm can be implemented using standard MATLAB commands with the model specifications. The most commonly used solvers for `cvx` is SeDuPi [52] and SDPT3 [53], which are interior-point optimization solvers. For this project the default SDPT3 solver was used. It is to be noted that `cvx` cannot be used to check if the problem is convex or not, but a basic knowledge about convex optimization is needed before using the solve the problem.

The algorithm in Chapter 3 Section 4-2 is revisited for convenience.

The highlighted `cvx` formulation in Algorithm 2 is examined below.

- `cvx_begin` – denotes the specification for the the new `cvx` formulation and allows the MATLAB to accept declaration of the variables, objective function and constraints of the problem.
- `variable` a_i – denotes a_i as the optimization variable. This a_i is used in the objective function.
- `minimize` $a_i = \|X_k * a_i - X_{k+1}\|_2^2 + \beta * \|a_i\|_1$ – denotes the objective function that is to be minimised. Here the LASSO problem in Equation 3-7 is implemented.
- `cvx_end` – denotes the end of `cvx` specification and that the problem is solved.

Algorithm 2 Algorithm for cvx to implement LASSO

Require: $\beta \geq 0$ **Ensure:** window size = 500 $\beta \leftarrow$ desired range of values $N \leftarrow$ length of β values $P \leftarrow$ length of total windows**for** $n \leftarrow 1$ to N **do** **for** $p \leftarrow 1$ to P **do** **for** $i \leftarrow 1$ to 128 **do** $a_i \leftarrow p^{th}(i, :)$

▷ number of channels

cvx_begin

 variable a_i $\beta \leftarrow$ variable n $X_k \leftarrow i^{th}$ data $X_{k+1} \leftarrow$ one step ahead predicted data minimize $a_i = \|X_k * a_i - X_{k+1}\|_2^2 + \beta * \|a_i\|_1$

cvx_end

end for **end for****end for**

Instruction to run a cvx block

For this thesis, the latest version of cvx was downloaded from <http://www.stanford.edu/~boyd/cvx>. The package needs to be initialized in the MATLAB in the following way [54].

- Open MATLAB
- Change the current directory in the MATLAB to be the location where the package was placed on the local computer.
- Type `cvx_setup` in command window of MATLAB. This allows MATLAB to access all the cvx package files and runs a test code to complete the installation with a No error message.
- Now run the cvx problem.

Appendix D

Statistical test

D-1 Two-sample Kolmogorov-Smirnov test

To validate that the distribution of eigenvalues through different anesthetic stages were not same, it was important to emphasize through a statistical test they were significantly different. Two-sample Kolmogorov-Smirnov test (K-S test) was used and their results were discussed in Chapter 4 in pages 38, 41, and 44. The statistical test aims to reject the null hypothesis, which implies that the alternate hypothesis is true. If the test fails to reject the null hypothesis, then this implies that the null hypothesis can no longer be accepted [55]. K-S test is a non-parametric test technique, which means that it is not a function of a parameter, but of a sample [55]. K-S test is defined as,

H_0 : The distribution of the vectors x and y are same (null hypothesis)

H_1 : The distribution of the vectors x and y are different (alternate hypothesis)

α (alpha) : 5% significance level.

Test statistic : Difference between the cumulative distribution function of the two vectors.

Null distribution means that the distribution of the test statistic under null hypothesis, where test statistic is the random variable calculated. Null hypothesis here refers to the condition or hypothesis where the difference between the two vectors is zero. Therefore, in K-S test, null distribution happens when the vectors are drawn from the same distribution itself.

Bibliography

- [1] P. Roussel, G. Le Godais, F. Bocquelet, M. Palma, J. Hongjie, S. Zhang, P. Kahane, S. Chabardès, and B. Yvert, “Acoustic contamination of electrophysiological brain signals during speech production and sound perception,” *BioRxiv*, p. 722207, 2019.
- [2] M. Styner, R. Knickmeyer, S. Joshi, C. Coe, S. J. Short, and J. Gilmore, “Automatic brain segmentation in rhesus monkeys,” in *Medical Imaging 2007: Image Processing*, vol. 6512, p. 65122L, International Society for Optics and Photonics, 2007.
- [3] G. A. Mashour, B. A. Orser, M. S. Avidan, and D. S. Warner, “Intraoperative Awareness: From Neurobiology to Clinical Practice,” *Anesthesiology*, vol. 114, pp. 1218–1233, 05 2011.
- [4] A. Ashourvan, S. Pequito, A. N. Khambhati, F. Mikhail, S. N. Baldassano, K. A. Davis, T. H. Lucas, J. M. Vettel, B. Litt, G. J. Pappas, *et al.*, “Model-based design for seizure control by stimulation,” *Journal of neural engineering*, vol. 17, no. 2, p. 026009, 2020.
- [5] G. Solovey, L. M. Alonso, T. Yanagawa, N. Fujii, M. O. Magnasco, G. A. Cecchi, and A. Proekt, “Loss of consciousness is associated with stabilization of cortical activity,” *Journal of Neuroscience*, vol. 35, no. 30, pp. 10866–10877, 2015.
- [6] T. A. Bowdle, “Depth of anesthesia monitoring,” *Anesthesiology Clinics of North America*, vol. 24, no. 4, pp. 793–822, 2006.
- [7] E. N. Brown, R. Lydic, and N. D. Schiff, “General anesthesia, sleep, and coma,” *New England Journal of Medicine*, vol. 363, no. 27, pp. 2638–2650, 2010.
- [8] E. N. Brown and F. J. Flores, “General Anesthesia Causes Telltale Brain activity Patterns,” *The Scientist Magazine*®, March 2019.
- [9] B. Musizza and S. Ribaric, “Monitoring the depth of anaesthesia,” *Sensors*, vol. 10, no. 12, pp. 10896–10935, 2010.
- [10] R. Sanders, G. Tononi, S. Laureys, J. Sleight, and D. Warner, “Unresponsiveness Unconsciousness,” *Anesthesiology*, vol. 116, pp. 946–959, 04 2012.

- [11] A. Agarwal and K. Kishore, "Complications and controversies of regional anaesthesia: a review," *Indian journal of anaesthesia*, vol. 53, no. 5, p. 543, 2009.
- [12] L. G. Braz, D. G. Braz, D. S. d. Cruz, L. A. Fernandes, N. S. P. Módolo, and J. R. C. Braz, "Mortality in anesthesia: a systematic review," *Clinics*, vol. 64, pp. 999–1006, 2009.
- [13] G. Schneider, D. Jordan, G. Schwarz, P. Bischoff, C. J. Kalkman, H. Kuppe, I. Rundshagen, A. Omerovic, M. Kreuzer, G. Stockmanns, *et al.*, "Monitoring depth of anesthesia utilizing a combination of electroencephalographic and standard measures," *Anesthesiology*, vol. 120, no. 4, pp. 819–828, 2014.
- [14] J. Bruhn, P. S. Myles, R. Sneyd, and M. M. Struys, "Depth of anaesthesia monitoring: what's available, what's validated and what's next?," *BJA: British Journal of Anaesthesia*, vol. 97, no. 1, pp. 85–94, 2006.
- [15] G. A. Dumont, A. Martinez, and J. M. Ansermino, "Robust control of depth of anesthesia," *International Journal of Adaptive Control and Signal Processing*, vol. 23, no. 5, pp. 435–454, 2009.
- [16] G. Northoff, S. Wainio-Theberge, and K. Evers, "Spatiotemporal neuroscience – what is it and why we need it," *Physics of Life Reviews*, vol. 33, pp. 78–87, 2020.
- [17] W. Huang, L. Goldsberry, N. F. Wymbs, S. T. Grafton, D. S. Bassett, and A. Ribeiro, "Graph frequency analysis of brain signals," *IEEE journal of selected topics in signal processing*, vol. 10, no. 7, pp. 1189–1203, 2016.
- [18] G. Solovey, K. J. Miller, J. Ojemann, M. O. Magnasco, and G. A. Cecchi, "Self-regulated dynamical criticality in human ECoG," *Frontiers in Integrative Neuroscience*, vol. 6, p. 44, 2012.
- [19] P. L. Purdon, E. T. Pierce, E. A. Mukamel, M. J. Prerau, J. L. Walsh, K. F. K. Wong, A. F. Salazar-Gomez, P. G. Harrell, A. L. Sampson, A. Cimenser, *et al.*, "Electroencephalogram signatures of loss and recovery of consciousness from propofol," *Proceedings of the National Academy of Sciences*, vol. 110, no. 12, pp. E1142–E1151, 2013.
- [20] A. Ashourvan, S. Pequito, A. N. Khambhati, S. N. Baldassano, K. A. Davis, T. Lucas, J. M. Vettel, B. Litt, G. J. Pappas, and D. S. Bassett, "Parsing spatiotemporal dynamical stability in ECoG during seizure onset, propagation, and termination," *arXiv preprint arXiv:1706.08202*, 2017.
- [21] J. F. Brosschot, B. Verkuil, and J. F. Thayer, "Conscious and unconscious perseverative cognition: Is a large part of prolonged physiological activity due to unconscious stress?," *Journal of psychosomatic research*, vol. 69, no. 4, pp. 407–416, 2010.
- [22] P. Garcia, M. K. Whalin, and P. S. Sebel, "Chapter 9 - Intravenous anesthetics," in *Pharmacology and Physiology for Anesthesia* (H. C. Hemmings and T. D. Egan, eds.), pp. 137–158, Philadelphia: W.B. Saunders, 2013.
- [23] A. Brancaccio, D. Tabarelli, M. Bigica, and D. Baldauf, "Cortical source localization of sleep-stage specific oscillatory activity," *Scientific reports*, vol. 10, no. 1, pp. 1–15, 2020.

-
- [24] D. M. Groppe, S. Bickel, C. J. Keller, S. K. Jain, S. T. Hwang, C. Harden, and A. D. Mehta, “Dominant frequencies of resting human brain activity as measured by the electrocorticogram,” *Neuroimage*, vol. 79, pp. 223–233, 2013.
- [25] B. He, L. Yang, C. Wilke, and H. Yuan, “Electrophysiological imaging of brain activity and connectivity—challenges and opportunities,” *IEEE transactions on biomedical engineering*, vol. 58, no. 7, pp. 1918–1931, 2011.
- [26] B. Burle, L. Spieser, C. Roger, L. Casini, T. Hasbroucq, and F. Vidal, “Spatial and temporal resolutions of EEG: Is it really black and white? a scalp current density view,” *International Journal of Psychophysiology*, vol. 97, no. 3, pp. 210–220, 2015.
- [27] N. J. Hill, D. Gupta, P. Brunner, A. Gunduz, M. A. Adamo, A. Ritaccio, and G. Schalk, “Recording human electrocorticographic (ECoG) signals for neuroscientific research and real-time functional cortical mapping,” *JoVE (Journal of Visualized Experiments)*, no. 64, p. e3993, 2012.
- [28] J. Parvizi and S. Kastner, “Human intracranial EEG: promises and limitations,” *Nature neuroscience*, vol. 21, no. 4, p. 474, 2018.
- [29] B. Graimann, G. Townsend, J. Huggins, A. Schlögl, S. Levine, and G. Pfurtscheller, “A comparison between using ECoG and EEG for direct brain communication,” *Proceedings of the EMBEC05*, 2005.
- [30] S. Haufe, P. DeGuzman, S. Henin, M. Arcaro, C. J. Honey, U. Hasson, and L. C. Parra, “Elucidating relations between fMRI, ECoG, and EEG through a common natural stimulus,” *NeuroImage*, vol. 179, pp. 79–91, 2018.
- [31] G. Smith, J. R. D’Cruz, B. Rondeau, and J. Goldman, “General anesthesia for surgeons,” *StatPearls [Internet]*, 2020.
- [32] A. Y. Feng, A. D. Kaye, R. J. Kaye, K. Belani, and R. D. Urman, “Novel propofol derivatives and implications for anesthesia practice,” *Journal of anaesthesiology, clinical pharmacology*, vol. 33, no. 1, p. 9, 2017.
- [33] H. Q. Ontario *et al.*, “Bispectral index monitor: an evidence-based analysis,” *Ont Health Technol Assess Ser*, vol. 4, no. 9, pp. 1–70, 2004.
- [34] E.-L. Zetterlund, H. Gréen, A. Oscarsson, S. Vikingsson, M. Vrethem, M.-L. Lindholm, and C. Eintrei, “Determination of loss of consciousness: a comparison of clinical assessment, bispectral index and electroencephalogram: An observational study,” *European Journal of Anaesthesiology/ EJA*, vol. 33, no. 12, pp. 922–928, 2016.
- [35] G. Solovey, K. J. Miller, J. Ojemann, M. O. Magnasco, and G. A. Cecchi, “Self-regulated dynamical criticality in human ECoG,” *Frontiers in Integrative Neuroscience*, vol. 6, p. 44, 2012.
- [36] S. Pequito, A. Ashourvan, D. Bassett, B. Litt, and G. J. Pappas, “Spectral control of cortical activity,” in *2017 American Control Conference (ACC)*, pp. 2785–2791, IEEE, 2017.

- [37] A. Roli, M. Villani, A. Filisetti, and R. Serra, “Dynamical criticality: overview and open questions,” *Journal of Systems Science and Complexity*, vol. 31, no. 3, pp. 647–663, 2018.
- [38] M. Botcharova, S. F. Farmer, and L. Berthouze, “Markers of criticality in phase synchronization,” *Frontiers in systems neuroscience*, vol. 8, p. 176, 2014.
- [39] A. Neumaier and T. Schneider, “Estimation of parameters and eigenmodes of multivariate autoregressive models,” *ACM Transactions on Mathematical Software (TOMS)*, vol. 27, no. 1, pp. 27–57, 2001.
- [40] C.-H. Juan, K. T. Nguyen, W.-K. Liang, A. J. Quinn, Y.-H. Chen, N. G. Muggleton, J.-R. Yeh, M. W. Woolrich, A. C. Nobre, and N. E. Huang, “Revealing the Dynamic nature of Amplitude Modulated Neural Entrainment with Holo-Hilbert Spectral Analysis,” *Frontiers in Neuroscience*, vol. 15, 2021.
- [41] L. M. Alonso, G. Solovey, T. Yanagawa, A. Proekt, G. A. Cecchi, and M. O. Magnasco, “Single-trial classification of awareness state during anesthesia by measuring critical dynamics of global brain activity,” *Scientific reports*, vol. 9, no. 1, pp. 1–11, 2019.
- [42] T. Yanagawa, Z. C. Chao, N. Hasegawa, and N. Fujii, “Large-scale information flow in conscious and unconscious states: an ECoG study in monkeys,” *PloS one*, vol. 8, no. 11, p. e80845, 2013.
- [43] L. M. Alonso, G. Solovey, T. Yanagawa, A. Proekt, G. A. Cecchi, and M. O. Magnasco, “Learning to read the imprints of consciousness on global brain dynamics: an application to intra-operative monitoring of anesthesia,” *bioRxiv*, p. 225813, 2017.
- [44] R. J. Rushmore, S. Bouix, M. Kubicki, Y. Rathi, D. L. Rosene, E. H. Yeterian, and N. Makris, “MRI-based Parcellation and Morphometry of the Individual Rhesus Monkey Brain: the macaque Harvard-Oxford Atlas (mHOA), a translational system referencing a standardized ontology,” *Brain imaging and behavior*, vol. 15, no. 3, pp. 1589–1621, 2021.
- [45] J.-F. Gariépy, K. K. Watson, E. Du, D. L. Xie, J. Erb, D. Amasino, and M. L. Platt, “Social learning in humans and other animals,” *Frontiers in neuroscience*, vol. 8, p. 58, 2014.
- [46] D. Purves, G. Augustine, D. Fitzpatrick, L. Katz, A. LaMantia, J. McNamara, and S. Williams, “Neuroscience 2nd edition. sunderland (ma) sinauer associates,” *Types of Eye Movements and Their Functions*, 2001.
- [47] R. Tibshirani, “Regression shrinkage and selection via the LASSO,” *Journal of the Royal Statistical Society: Series B (Methodological)*, vol. 58, no. 1, pp. 267–288, 1996.
- [48] L. Kirkland, F. Kanfer, and S. Millard, “LASSO tuning parameter selection,” pp. 49–56, 12 2015.
- [49] J. A. Hartigan and M. A. Wong, “Algorithm as 136: A k-means clustering algorithm,” *Journal of the royal statistical society. series c (applied statistics)*, vol. 28, no. 1, pp. 100–108, 1979.
- [50] A. Likas, N. Vlassis, and J. J. Verbeek, “The global k-means clustering algorithm,” *Pattern recognition*, vol. 36, no. 2, pp. 451–461, 2003.

-
- [51] A. Neumaier and T. Schneider, “Estimation of parameters and eigenmodes of multivariate autoregressive models,” *ACM Transactions on Mathematical Software (TOMS)*, vol. 27, no. 1, pp. 27–57, 2001.
- [52] J. F. Sturm, “Using SeDuMi 1.02, a MATLAB toolbox for optimization over symmetric cones,” *Optimization methods and software*, vol. 11, no. 1-4, pp. 625–653, 1999.
- [53] K. Toh, R. Tütüncü, and M. Todd, “SDPT3 4.0 (beta)(software package),” tech. rep., Technical report, Department of Mathematics National University of Singapore, 2006.
- [54] M. Grant, S. Boyd, and Y. Ye, “cvx users’ guide,” *online: <http://www.stanford.edu/~boyd/software.html>*, 2009.
- [55] I. M. Chakravarti, R. G. Laha, and J. Roy, “Handbook of methods of applied statistics,” *Wiley Series in Probability and Mathematical Statistics (USA) eng*, 1967.

Glossary

List of Acronyms

GA	General Anesthesia
DoA	depth of anesthesia
ECoG	electrocorticography
EEG	electroencephalograph
LASSO	least absolute shrinkage and selection operator
AR	Auto regressive
CNS	central nervous system
BIS	Bispectral

List of Symbols

β	Tuning parameter
δ	Sampling frequency
λ	Eigenvalue
A	State matrix or coupling matrix
F_s	Sampling frequency

